

Logarithmic link smearing for full QCD

Stephan Dürr

Universität Bern, Institut für theoretische Physik, Sidlerstr. 5, CH-3012 Bern, Switzerland

Abstract

A Lie-algebra based recipe for smoothing gauge links in lattice field theory is presented, building on the matrix logarithm. With or without hypercubic nesting, this LOG/HYL smearing yields fat links which are differentiable w.r.t. the original ones. This is essential for defining UV-filtered (“fat link”) fermion actions which may be simulated with a HMC-type algorithm. The effect of this smearing on the distribution of plaquettes and on the residual mass of tree-level $O(a)$ -improved clover fermions in quenched QCD is studied.

1 Introduction

In lattice field theory one is generally interested in taking the continuum limit where the lattice spacing a tends to zero. In other words, one calculates the ratio $R(a)$ of two physical masses or matrix elements and considers the limit where the correlation length in lattice units diverges, $\xi/a \rightarrow \infty$. Since the physical box volume is supposed to be roughly constant, the total number of variables (and hence the CPU time needed) grows with a large power of a^{-1} .

To speed up the computation of the continuum ratio two concepts have proven important. The first one is known as Symanzik improvement [1]. Here one augments both the action and the observable by irrelevant terms. Upon tuning some coefficients it may be achieved that the continuum value is approached at a quadratic rate, $R(a) = R(0) + \text{const} (a/r_0)^2 + O(a^3)$, rather than linearly, $R(a) = R(0) + \text{const} a/r_0 + O(a^2)$, where r_0 is a fixed length. Hence, if the Symanzik scaling window (the regime where the “const” term dominates) starts at $a \simeq 0.1$ fm and one wishes to cover three quarters of the variable in which one extrapolates linearly, the finest lattice will have $a \simeq 0.05$ fm with improvement versus $a \simeq 0.025$ fm without.

The second ingredient in today's state-of-the-art simulations is some damping of ultra-violet (UV) fluctuations, that is of unphysical excitations at the scale of the cut-off a^{-1} . To maintain locality, such damping is achieved via locally averaging field variables. In case of a gauge theory one replaces the link $U_\mu(x)$, the parallel transporter from $x+\hat{\mu}$ to x , by $U'_\mu(x)$. The latter is some average of paths, attached to the same endpoints, which stay within a local neighborhood of x and $x+\hat{\mu}$. From a formal viewpoint such smearing amounts to another change of the action by irrelevant terms; thus changing “const” in the extrapolation law, but not the power (i.e. the Symanzik class is unchanged). Data suggest that some mild smearing enlarges the scaling window and reduces the “const” (in absolute magnitude) in the extrapolation law [2, 3].

Specifically for lattice QCD it has been observed that these two strategies, when applied together, enhance each others effectiveness. With staggered quarks this has been demonstrated in a somewhat indirect manner. Upon combining a Naik term with a specific UV-filtering known as “AsqTad” smearing the MILC collaboration has been able to simulate large volumes with standard lattice spacings and fairly light pion masses [4]. For fat-link clover quarks [2] the

enhancement has been investigated in detail in the quenched approximation [5], and there is a similar program for large-scale dynamical simulations with almost-realistic quark masses [6].

What remains is an engineering issue. With the smearing being part of the action or operator definition, it seems natural to keep the parameter α and the iteration level n_{iter} unchanged as the lattice spacing is reduced. This way locality is guaranteed, and $(\alpha, n_{\text{iter}})$ represents a handle to influence the overall cost, while the ratio $R(0)$ is, ultimately, unchanged. Of course one may ask what is the “optimal” choice of $(\alpha, n_{\text{iter}})$, in terms of CPU time, to achieve a predefined accuracy of $R(0)$. In practice, however, one is interested in the continuum limit for a number of quantities, and often this list enlarges as the simulation program progresses. Thus, staying away from either extreme choice (i.e. no or excessive smearing) will often be sufficient.

For theories with dynamical fermions an additional engineering constraint emerges. There is a single algorithm which scales, at fixed bare parameters, almost linearly with the box volume, known as hybrid Monte Carlo algorithm (HMC), with subvarieties called PHMC, RHMC [7]. This algorithm demands that the fermion action reacts smoothly to a change of the field of gauge variables $U_\mu(x)$. For fat-link actions this requires that the smeared link $U'_\mu(x)$ be differentiable with respect to $U_\mu(x)$, which amounts to a constraint on the smearing recipe.

Historically, the first smoothing introduced has been APE smearing [8]

$$U_\mu^{\text{APE}}(x) = P_{SU(3)} \left\{ (1 - \alpha) U_\mu(x) + \frac{\alpha}{2(d-1)} \sum_{\pm\nu \neq \mu} U_\nu(x) U_\mu(x + \hat{\nu}) U_\nu^\dagger(x + \hat{\mu}) \right\} \quad (1)$$

$$= P_{SU(3)} \left\{ (1 - \alpha) I + \frac{\alpha}{2(d-1)} \sum_{\pm\nu \neq \mu} U_\nu(x) U_\mu(x + \hat{\nu}) U_\nu^\dagger(x + \hat{\mu}) U_\mu^\dagger(x) \right\} U_\mu(x) \quad (2)$$

with P_G denoting the projection to the gauge group G . The rewriting in the second line is based on $P_{SU(3)}\{AU\} = P_{SU(3)}\{A\}U$, valid for the combination of an arbitrary matrix A and a special unitary U . Since the $U(1)$ projection [cf. (49, 50) below for details] creates a headache in the HMC force, Morningstar and Peardon invented the “stout” smearing [9]

$$U_\mu^{\text{EXP}}(x) = \exp \left(\frac{\alpha}{2} \sum_{\pm\nu \neq \mu} \left\{ [U_\nu(x) U_\mu(x + \hat{\nu}) U_\nu^\dagger(x + \hat{\mu}) U_\mu^\dagger(x) - \text{h.c.}] - \frac{1}{3} \text{Tr}[\cdot] \right\} \right) U_\mu(x) \quad (3)$$

subsequently dubbed EXP, which, by design, yields differentiable fat links. However, it turns out that (3) is less effective in damping extremal plaquettes than (2). In Ref. [10] a modified nAPE smearing has been introduced where the projection is to $U(3)$ only. The goal of this article is to test yet another smearing which yields an $SU(3)$ valued differentiable link, with an efficient damping of the UV fluctuations, such that it could be used in full QCD.

This article is organized as follows. The next two sections specify the new LOG smearing and show how it can be used together with the hypercubic nesting trick, defining the HYL smearing. Sections 4 and 5 investigate the impact on selected observables, in particular the distribution of plaquettes and the residual mass of fat-clover fermions. In the latter case evidence is given that $M_\pi \simeq 160$ MeV can be reached at standard β -values in $O(a)$ -improved quenched QCD without hitting the so-called “exceptional configuration” problem. Sections 6 and 7 sketch how the LOG/HYL smearing is included in a HMC approach to full QCD and how the matrix logarithm may be used to define a new gauge action and the pertinent (gluonic) topological charge density. After a summary, three appendices give technical details.

2 Logarithmic link smearing

The re-written form (2) of the APE smearing contains the factor $P_{SU(3)}\{.\}$ by which the original link $U_\mu(x)$ is multiplied. Upon sending the parameter $\alpha \rightarrow 0$ this prefactor is smoothly deformed into unity. If one wishes to stay in the group, the backprojection is needed, since the weighted arithmetic average of the identity and six (in 4D) “blades” (closed staples) is not a group element any more. Given the standard definition of the fractional power of a matrix

$$U^\alpha = \exp(\alpha \log(U)) \quad (4)$$

one starts wondering whether it would make sense to define the smeared link as

$$U'_\mu(x) = \exp\left(\frac{\alpha}{2(d-1)} \sum_{\pm\nu \neq \mu} \log[U_\nu(x)U_\mu(x+\hat{\nu})U_\nu^\dagger(x+\hat{\mu})U_\mu^\dagger(x)]\right) U_\mu(x) \quad (5)$$

and on a sufficiently smooth gauge background the rationale for this choice is as follows. The product $U_\nu(x)U_\mu(x+\hat{\nu})U_\nu^\dagger(x+\hat{\mu})U_\mu^\dagger(x)$ is special unitary, its logarithm thus anti-hermitean and traceless. So is the sum, and this means that the exponential defines again a special unitary matrix which is to be multiplied onto the original link. Hence one stays in $SU(3)$.

The problem is that the argument has a loophole: On an arbitrary gauge configuration the logarithm is *not* traceless, it is just traceless modulo $2\pi i$. Upon averaging this logarithm with the remaining five (in 4D) contributions, which we assume to be traceless, one gets an arbitrary trace. As a result, the exponential is still unitary, but its determinant is not 1, so one leaves the gauge group. While, even on a rough configuration, $\text{Tr} \log[U_\nu(x)U_\mu(x+\hat{\nu})U_\nu^\dagger(x+\hat{\mu})U_\mu^\dagger(x)] \neq 0$ is rare, if one wishes to stay in $SU(3)$, this possibility needs to be accounted for.

Obviously, by restricting the sum to traceless contributions, the goal of staying in the gauge group is reached. The most straightforward option is to define the smearing through

$$U''_\mu(x) = \exp\left(\frac{\alpha}{2(d-1)} \sum_{\pm\nu \neq \mu} \left\{ \log[U_\nu(x)U_\mu(x+\hat{\nu})U_\nu^\dagger(x+\hat{\mu})U_\mu^\dagger(x)] - \frac{1}{3} \text{Tr} \log[.] \right\}\right) U_\mu(x) \quad (6)$$

where, as mentioned before, the new term $-\frac{1}{3} \text{Tr} \log[.]$ is almost always zero. In tangent space the logarithm of the 4-link product may be decomposed as $\log[.] = \sum_{a=1}^8 i\xi^a T^a + i\xi^9 I$ with $\xi^a \in \mathbf{R}$ for $a = 1, \dots, 8$ and $\xi^9 \in \{0, \pm 2\pi/3\}$. Here, $T^a = \lambda^a/2$ with λ^a the Gell-Mann matrices. In (6) the 9th (radial) component is simply projected away, and after this correction, the six contributions to the tangent space are again subject to an arithmetic average.

A more general approach may allow for unequal weights of the six staples, depending on whether their logarithm is traceless or not. Hence, a more sophisticated version is

$$U'''_\mu(x) = \exp\left(\frac{\alpha}{2(d-1)} \sum_{\pm\nu \neq \mu} c_{\pm\nu} \left\{ \log[U_\nu(x)U_\mu(x+\hat{\nu})U_\nu^\dagger(x+\hat{\mu})U_\mu^\dagger(x)] - \frac{1}{3} \text{Tr} \log[.] \right\}\right) U_\mu(x) \quad (7)$$

where the coefficient $c_{\pm\nu}$ is a function of $\log[U_\nu(x)U_\mu(x+\hat{\nu})U_\nu^\dagger(x+\hat{\mu})U_\mu^\dagger(x)]$, for instance $c_\nu = +1$ if $\text{Tr} \log[.] = 0$ and $c_\nu = -0.5$ if $\text{Tr} \log[.] = \pm 2\pi i$. Still, in view of the application as an ingredient in a HMC, this definition seems less attractive, since it entails a rather complicated force.

Finally, one may choose to invoke a non-principal logarithm. In fact, thinking in terms of the eigenvalues λ_i of the original matrix (which we assume to be special unitary) it is natural to attribute a possible occurrence of $\text{Tr} \log[.] = +2\pi i$ to the λ_i with the largest imaginary part of

$\log(\lambda_i)$ (and ditto to the one with the smallest imaginary part of $\log(\lambda_i)$ for $\text{Tr} \log[\cdot] = -2\pi i$). Accordingly, a “trace-free” matrix logarithm may be defined which basically shifts the logarithm of one eigenvalue of the original matrix by $\pm 2\pi i$ in those cases where the principal logarithm has non-zero trace. With this function at hand, we define

$$U_\mu^{\text{LOG}}(x) = \exp\left(\frac{\alpha}{2(d-1)} \sum_{\pm\nu \neq \mu} \text{tflog}[U_\nu(x)U_\mu(x+\hat{\nu})U_\nu^\dagger(x+\hat{\mu})U_\mu^\dagger(x)]\right) U_\mu(x) \quad (8)$$

and below, whenever referring to the LOG recipe without specification, the recipe (8) will be meant. This “trace-free” logarithm seems most interesting, because in full QCD this version amounts to a smooth adaptation of the definition to the actual gauge field, which has a good chance to avoid large HMC forces. For implementation details of all varieties see App. A.

The construct (8) retains all symmetry properties of the original link, in particular the behavior under gauge transformations, charge conjugation, reflections, and permutations of the coordinate axes. It produces a link in $SU(3)$, with an obvious generalization to $SU(N_c)$, and the new $U_\mu^{\text{LOG}}(x)$ is differentiable with respect to the original $U_\mu(x)$. The normalization of the parameter α , which determines the weight of the fluctuation, has been chosen such that in leading order perturbation theory the new LOG recipe (8) agrees with the APE recipe (2). The same holds true for the stout/EXP recipe (3) if an extra factor $1/(2(d-1))$ is included [5].

3 Hypercubic nesting trick

To tame the noise in QCD observables, one would like to iterate the smearing, while keeping the delocalizing effect minimal. A nice strategy (inspired by the fixed-point action approach and the pertinent “perfect smearing”) was presented in [11]. In this original form the hypercubic nesting trick uses the APE smearing (2) as core recipe, giving

$$\begin{aligned} \bar{V}_{\mu,\nu\rho}(x) &= P_{SU(3)} \left\{ (1-\alpha_3)I + \frac{\alpha_3}{2} \sum_{\pm\sigma \neq \mu,\nu,\rho} U_\sigma(x) U_\mu(x+\hat{\sigma}) U_\sigma^\dagger(x+\hat{\mu}) U_\mu^\dagger(x) \right\} U_\mu(x) \\ \tilde{V}_{\mu,\nu}(x) &= P_{SU(3)} \left\{ (1-\alpha_2)I + \frac{\alpha_2}{4} \sum_{\pm\rho \neq \mu,\nu} \bar{V}_{\rho,\mu\nu}(x) \bar{V}_{\mu,\nu\rho}(x+\hat{\rho}) \bar{V}_{\rho,\mu\nu}^\dagger(x+\hat{\mu}) U_\mu^\dagger(x) \right\} U_\mu(x) \\ U_\mu^{\text{HYP}}(x) &= P_{SU(3)} \left\{ (1-\alpha_1)I + \frac{\alpha_1}{6} \sum_{\pm\nu \neq \mu} \tilde{V}_{\nu,\mu}(x) \tilde{V}_{\mu,\nu}(x+\hat{\nu}) \tilde{V}_{\nu,\mu}^\dagger(x+\hat{\mu}) U_\mu^\dagger(x) \right\} U_\mu(x) \quad (9) \end{aligned}$$

where we stick to the notation of [11] in which α_1 denotes the fluctuation weight in the *last* step. This has been generalized to the case of “stout/EXP” smearing [5] and in complete analogy

$$\begin{aligned} \bar{V}_{\mu,\nu\rho}(x) &= \exp\left(\frac{\alpha_3}{2} \sum_{\pm\sigma \neq \mu,\nu,\rho} \text{tflog}[U_\sigma(x) U_\mu(x+\hat{\sigma}) U_\sigma^\dagger(x+\hat{\mu}) U_\mu^\dagger(x)]\right) U_\mu(x) \\ \tilde{V}_{\mu,\nu}(x) &= \exp\left(\frac{\alpha_2}{4} \sum_{\pm\rho \neq \mu,\nu} \text{tflog}[\bar{V}_{\rho,\mu\nu}(x) \bar{V}_{\mu,\nu\rho}(x+\hat{\rho}) \bar{V}_{\rho,\mu\nu}^\dagger(x+\hat{\mu}) U_\mu^\dagger(x)]\right) U_\mu(x) \\ U_\mu^{\text{HYL}}(x) &= \exp\left(\frac{\alpha_1}{6} \sum_{\pm\nu \neq \mu} \text{tflog}[\tilde{V}_{\nu,\mu}(x) \tilde{V}_{\mu,\nu}(x+\hat{\nu}) \tilde{V}_{\nu,\mu}^\dagger(x+\hat{\mu}) U_\mu^\dagger(x)]\right) U_\mu(x) \quad (10) \end{aligned}$$

is the hypercubically nested version of LOG smearing. With these formulae given, all aspects of logarithmic link smearing have been specified and we are ready for a numerical investigation.

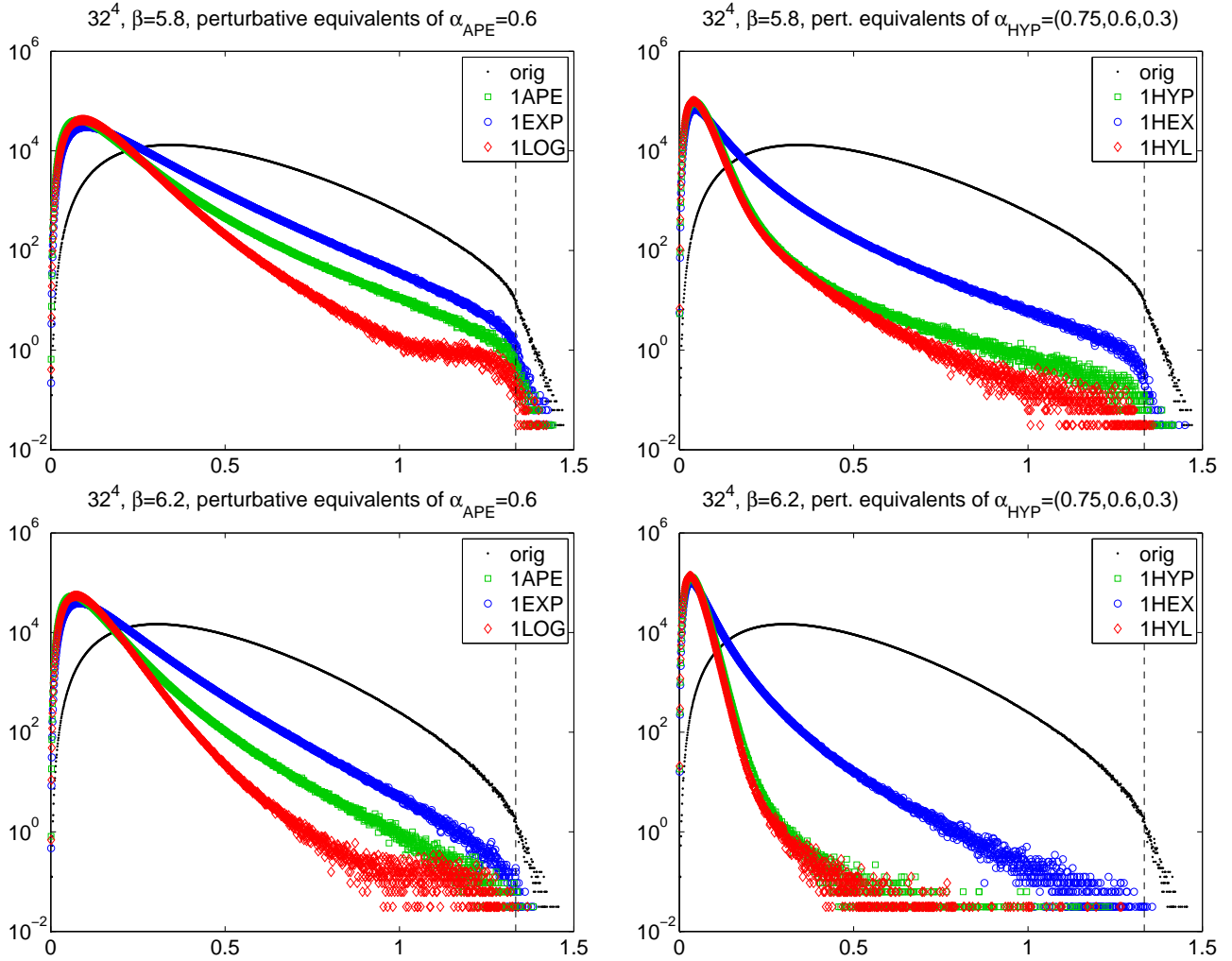


Figure 1: *Distribution of the plaquette on a 32^4 lattice at $\beta = 5.8$ (top) and $\beta = 6.2$ (bottom) after one step of APE/EXP/LOG smearing (left) or HYP/HEX/HYL smearing (right). To the right of the dashed line at $s = 4/3$ the non-principal definition of the log may prove relevant. Throughout perturbative equivalents of $\alpha_{\text{APE}} = 0.6$ and $\alpha_{\text{HYP}} = (0.75, 0.6, 0.3)$ have been used.*

4 Effect on selected gluonic observables

The LOG/HYL smearing (8, 10) may be used both in gluonic observables (e.g. for a fat-link topological charge or Polyakov loop) and in fermionic observables (e.g. for a fat-link Dirac operator). This section is devoted to the effect on one quantity in the pure gauge theory, the distribution of the plaquette. The comparison between the different smearing recipes will be organized both in an unfair manner (sticking to the perturbative equivalence rule described in Sect. 2) and in a fair way (using optimized parameters in each recipe).

Fig. 1 shows the distribution of the plaquette variable $s_{\mu\nu}(x) = 1 - \text{Re Tr}(U_{\mu\nu}(x))/3$ on a 32^4 grid in a pure gauge ensemble with the Wilson action at $\beta = 5.8$ and $\beta = 6.2$. The distribution vaguely resembles a black body radiation curve – it starts out with a power law and ends with a more-or-less exponential tail which, at not-so-large β is affected by the fact that $s \leq 1.5$. Smearing shifts the distribution towards a “colder” temperature, in particular the probability

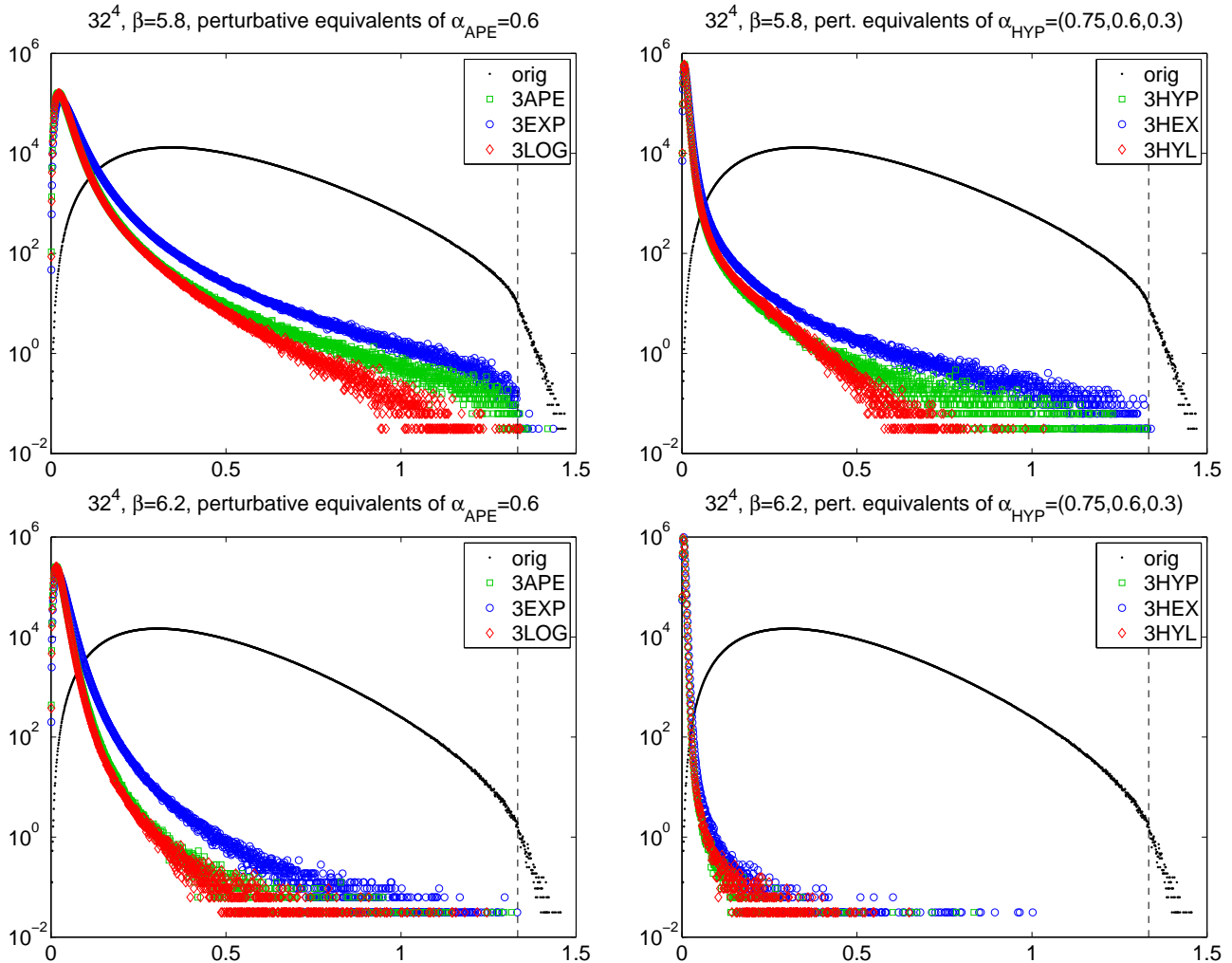


Figure 2: *The same as in Fig. 1, but after three iterations of the smearing have been applied.*

of large or extremal plaquettes is suppressed. Taking APE smearing as a standard, EXP (alias “stout”) is somewhat less effective, while the new LOG smearing is at least as effective. In this comparison perturbatively equivalent parameters have been used, that is $\alpha_{\text{APE}} = \alpha_{\text{LOG}} = 0.6$ and $\alpha_{\text{EXP}} = 0.1$ (see [5] for details). In the right panel a similar comparison is given for one step of HYP, HEX or HYL smearing. Again the perturbatively equivalent parameter set $\alpha_{\text{HYP}} = \alpha_{\text{HYL}} = (0.75, 0.6, 0.3)$ and $\alpha_{\text{HEX}} = (0.125, 0.15, 0.15)$ has been used, and with this specific choice HYP and HYL are more efficient than HEX. The two lower panels show that the difference between the smearings is reduced as β increases, in particular with the hypercubic nesting trick in place.

Fig. 2 shows the same distributions as Fig. 1, but this time after three iterations of the smearing. Again, APE and LOG are more effective than EXP, and HYP and HYL are better than HEX, albeit the difference seems less pronounced than in the previous figure.

In these figures the “trace-free” logarithm has been used. It turns out that the principal logarithm (5) yields an even better suppression of extremal plaquettes, but for reasons discussed in Sect. 2 the “trace-free” version seems more promising for an application in full QCD, and I have chosen to consistently show the results for this non-principal logarithm.

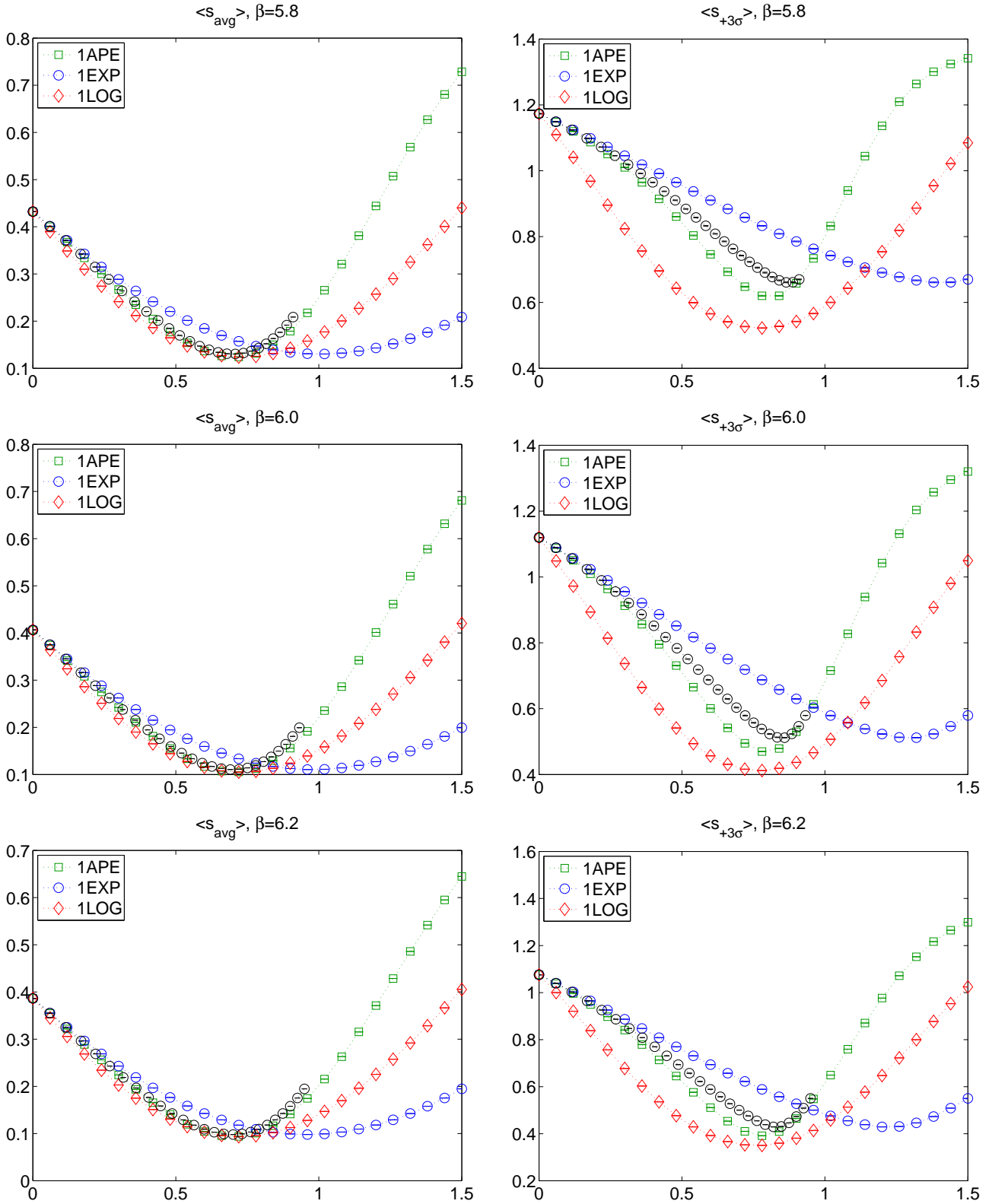


Figure 3: Average action s (left) and median-plus-3 σ -percentile of s (right) at $\beta = 5.8, 6.0, 6.2$ (from top to bottom) versus smearing parameter α , after 1 iteration of APE/EXP/LOG smoothing. To make the three α commensurate, the perturbative equivalence rule has been used, but the 1EXP data have also been redrawn as a function of α_{eff} as defined in (11).

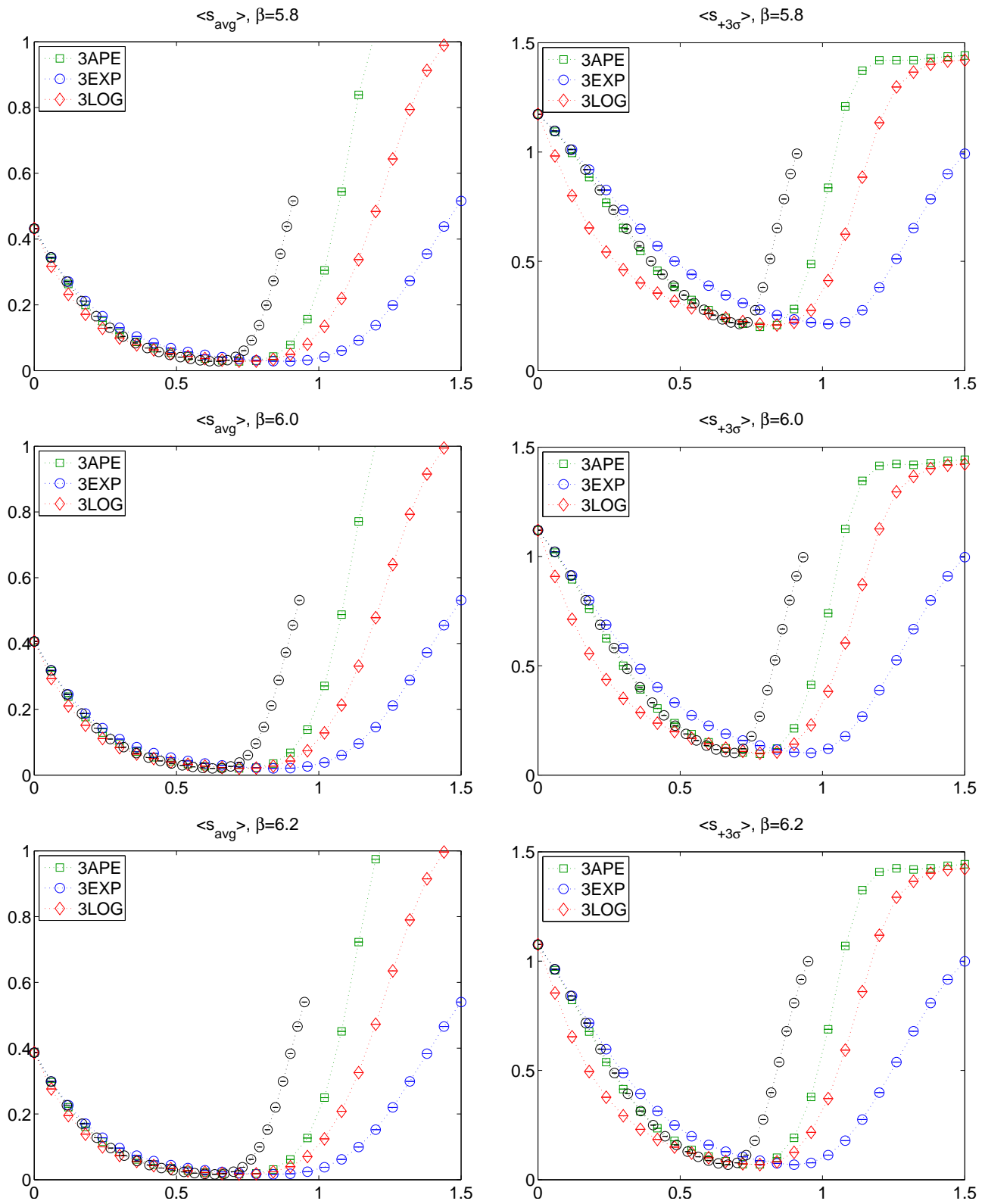


Figure 4: Same as Fig. 3, except that the effect of 3 iterations of APE/EXP/LOG smoothing is shown. The 3EXP data have been redrawn as a function of α_{eff} , as defined in (11), with $\langle P \rangle$ denoting the plaquette of the original (unsmearred) configuration.

Evidently, a fair comparison should use “optimized” values for each smearing. However, it is not so clear which quantity could be used in the optimization. For instance, statements about the effect of smearing on both the average plaquette and extremal plaquettes are found in the literature [11]. Moreover, once a specific quantity to optimize for has been selected, at least two characteristics should enter the comparison:

- (i) The value of the selected observable in the extremum.
- (ii) The width of the “near-minimal” region, i.e. whether the optimal smearing effect requires a fine-tuning of the parameters or whether any “near-optimal” choice will do fine, too.

To address these questions a scan over different smearing parameters in the APE/EXP/LOG recipes has been performed. The focus has been on the average plaquette s_{avg} and an “extremal” plaquette, here defined through $s_{+3\sigma}$ which is meant to denote the 0.99865 percentile, rather than s_{max} which is rather noisy. Data for $\beta = 5.8, 6.0, 6.2$ are collected in Figs. 3 and 4 for 1 and 3 iterations, respectively. All results are plotted as a function of $\alpha_{\text{APE}}, 6\alpha_{\text{EXP}}, \alpha_{\text{LOG}}$, but following the suggestion of [10] the EXP/stout data are also plotted as a function of

$$\alpha_{\text{eff}} = \frac{6\alpha_{\text{EXP}}}{1 + 6\alpha_{\text{EXP}}(1 - \langle P \rangle)} \quad (11)$$

where $\langle P \rangle$ denotes the plaquette (i.e. $1 - s$) of the original (unsmearing) configuration.

Regarding point (i), from Fig. 3 it is evident that the minimum of the average plaquette action is almost the same with all three smearings. Only the position at which it is assumed is somewhat different with EXP (it seems $\alpha \simeq 0.7$ is optimal for APE and LOG, and $6\alpha \simeq 1$ is a good choice for EXP), but most of this effect is gone if the latter data are plotted as a function of α_{eff} [10]. On the other hand, the “extremal” plaquette is quite sensitive to the details of the smearing recipe (right panel). With this criterion LOG smearing is significantly better than APE, and the latter is slightly more effective than EXP. However, this advantage diminishes towards large β , and also for higher iteration counts as Fig. 4 shows.

Regarding point (ii), we learn from Fig. 3 (right panel) that again LOG smearing has a slight advantage over the other two in showing a broader shape in the “near-minimal” region. In other words, this recipe seems more robust w.r.t. the details of the smearing parameter, in particular if an observable is chosen which is sensitive to near-extremal plaquettes. Again, larger β -values and higher iteration counts tend to diminish the effect.

5 Effect on selected fermionic observables

The main rationale for the LOG/HYL smearing (8, 10) has been to create a smearing that may be used as an ingredient in a fermion action suitable for full QCD simulations with the HMC algorithm. Therefore it is important to test a fat-link fermion with this kind of smearing and to compare it to similar actions where APE/HYP or EXP/HEX smearing has been used. This may be done with Wilson or with staggered quarks. In the former case the focus should be on chiral symmetry breaking, in the latter case on taste symmetry violation. For definiteness, I concentrate on Wilson fermions (with a clover term) and I choose the simplest observable sensitive to chiral symmetry violation: I measure the residual mass m_{res} , defined as the PCAC mass at bare mass $m_0 = 0$. Lacking the CPU power needed to simulate full QCD, I choose the quenched theory as testing ground. In fact, from an engineering viewpoint this choice is likely

$(\beta, L/a)$	(5.6, 08)	(5.8, 12)	(6.0, 16)	(6.2, 22)	(6.4, 28)
L/r_0	3.48	3.27	2.98	2.98	2.87
$a^{-1}[\text{GeV}]$	0.908	1.45	2.12	2.91	3.84
n_conf	256	128	64	32	16
1 APE	0.4367(20)	0.2607(11)	0.1931(06)	0.1589(04)	0.1371(03)
1 HYP	0.1914(13)	0.0937(09)	0.0615(05)	0.0490(02)	0.0421(02)
1 EXP	0.5470(24)	0.3400(14)	0.2572(08)	0.2129(06)	0.1838(03)
1 HEX	0.3146(18)	0.1583(10)	0.1030(05)	0.0784(03)	0.0641(02)
1 LOG	0.4309(20)	0.2570(11)	0.1905(06)	0.1569(04)	0.1355(03)
1 HYL	0.1923(13)	0.0929(08)	0.0606(05)	0.0482(02)	0.0414(02)
3 APE	0.1949(14)	0.0850(10)	0.0489(06)	0.0354(03)	0.0285(02)
3 HYP	0.0681(11)	0.0242(09)	0.0109(06)	0.0069(03)	0.0053(02)
3 EXP	0.2368(16)	0.1075(10)	0.0636(06)	0.0462(03)	0.0369(02)
3 HEX	0.0950(13)	0.0305(10)	0.0128(07)	0.0078(03)	0.0059(02)
3 LOG	0.1972(14)	0.0858(10)	0.0492(06)	0.0357(03)	0.0287(03)
3 HYL	0.0696(11)	0.0247(09)	0.0110(07)	0.0068(03)	0.0053(02)
7 HYL	0.0303(08)	0.0109(06)	0.0040(05)	0.0020(02)	0.0014(01)

Table 1: Residual mass am_{res} , defined as the PCAC quark mass at zero bare mass, for various couplings and smearings. The box geometry is $L^3 \times T$ with $T=2L$, and errors are statistical.

to be more indicative of the quality of the smearing, since there is no determinant which would mitigate the effect of spurious almost-zero modes.

With standard conventions the ($r=1$) Wilson operator takes the form

$$D_{\text{W}}(x, y) = \frac{1}{2} \sum_{\mu} \left\{ (\gamma_{\mu} - I) U_{\mu}(x) \delta_{x+\hat{\mu}, y} - (\gamma_{\mu} + I) U_{\mu}^{\dagger}(x - \hat{\mu}) \delta_{x-\hat{\mu}, y} \right\} + \frac{1}{2\kappa} \delta_{x, y} \quad (12)$$

with I a 4×4 spinor matrix and $1/(2\kappa) = 4 + m_0$. The Sheikholeslami-Wohlert clover operator follows by subtracting a hermitean contribution proportional to the gauge field strength [12]

$$D_{\text{SW}}(x, y) = D_{\text{W}}(x, y) - \frac{c_{\text{SW}}}{2} \sum_{\mu < \nu} \sigma_{\mu\nu} F_{\mu\nu} \delta_{x, y} \quad (13)$$

with $\sigma_{\mu\nu} = \frac{i}{2} [\gamma_{\mu}, \gamma_{\nu}]$ and $F_{\mu\nu}$ the hermitean clover-leaf operator. The same kind of UV-filtering is applied to the covariant derivative and to the clover term. In other words, the gauge link $U_{\mu}(x)$ in (12) is replaced, for instance, by $U_{\mu}^{\text{LOG}}(x)$ and the field-strength tensor $F_{\mu\nu}(x)$ in (13) is built from such links, too (see [5] for references to other options). Throughout, the tree-level improvement coefficient $c_{\text{SW}} = 1$ is used. The goal is to test the smearings and to compare the non-perturbative data to the perturbative 1-loop prediction for m_{res} .

The details of the gauge configurations can be read off from the heading of Tab. 1. The box geometry is $L^3 \times T$ with $T=2L$. The five couplings between $\beta = 5.6$ and $\beta = 6.4$ and the grid sizes have been chosen such that the physical box volumes are approximately equal, aiming for $L/r_0 \simeq 3$ by the formula for $r_0(\beta)$ from [13]. The values in the $a^{-1}[\text{GeV}]$ line are based on the assumption $r_0 = 0.5 \text{ fm}$ and indicate that the lattice spacing varies by a factor 4. A point- or $U(1)$ wall source has been used, and the point-sink has been averaged over the time-slice. The inversion of the clover operator has been performed with an even-odd preconditioned version of the biconjugate gradient γ_5 algorithm (BCG γ_5), with details given in App. B.

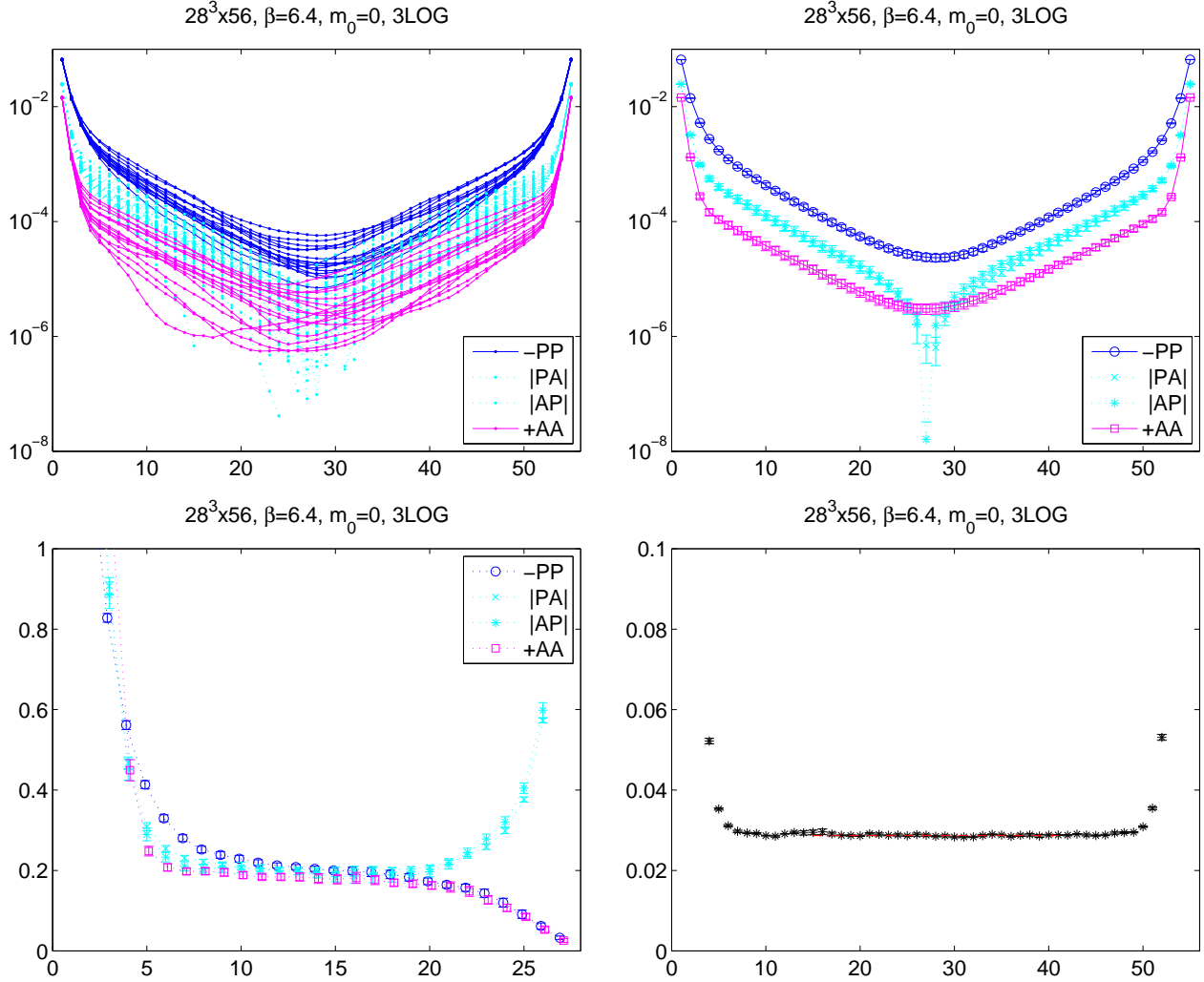


Figure 5: Individual and averaged pion correlators at $\beta = 6.4$ and $am_0 = 0$ with 3LOG steps, together with resulting pion mass and PCAC mass (everything in lattice units).

An illustration of the observables studied is given in Fig. 5, based on the run at $\beta = 6.4$ with the 3LOG action. Using both $\bar{\psi}\gamma_5\psi$ and $\bar{\psi}\gamma_4\gamma_5\psi$ as interpolating fields the direct and crossed correlators have been calculated, labeled as “PP”, “AA” and “PA/AP”, respectively. The individual correlators and the pertinent ensemble averages are shown in the first and second panel. The third plot indicates the resulting effective masses for M_π . The pion mass seems to be around $M_\pi \simeq 0.17a^{-1} = 650$ MeV, but the box is not sufficiently long to see a good plateau. Finally, the fourth plot contains the plateau of the PCAC mass, the latter being defined as

$$am^{\text{PCAC}} = \frac{(\partial_4 + \partial_4^*)\langle A(x)P(0) \rangle}{4\langle P(x)P(0) \rangle}. \quad (14)$$

In Fig. 6 the same observables are shown (again at $\beta = 6.4$) for the action with 3HYL steps. Evidently, with $am_0 = 0$ kept fixed, the pion is much lighter now. By comparing the first two plots to their counterparts in Fig. 5 one sees that the correlators are much fuzzier now. In consequence, the effective mass plot for M_π does not show a good plateau at all. Luckily, the PCAC mass is still easy to determine, and this is sufficient for the present investigation.

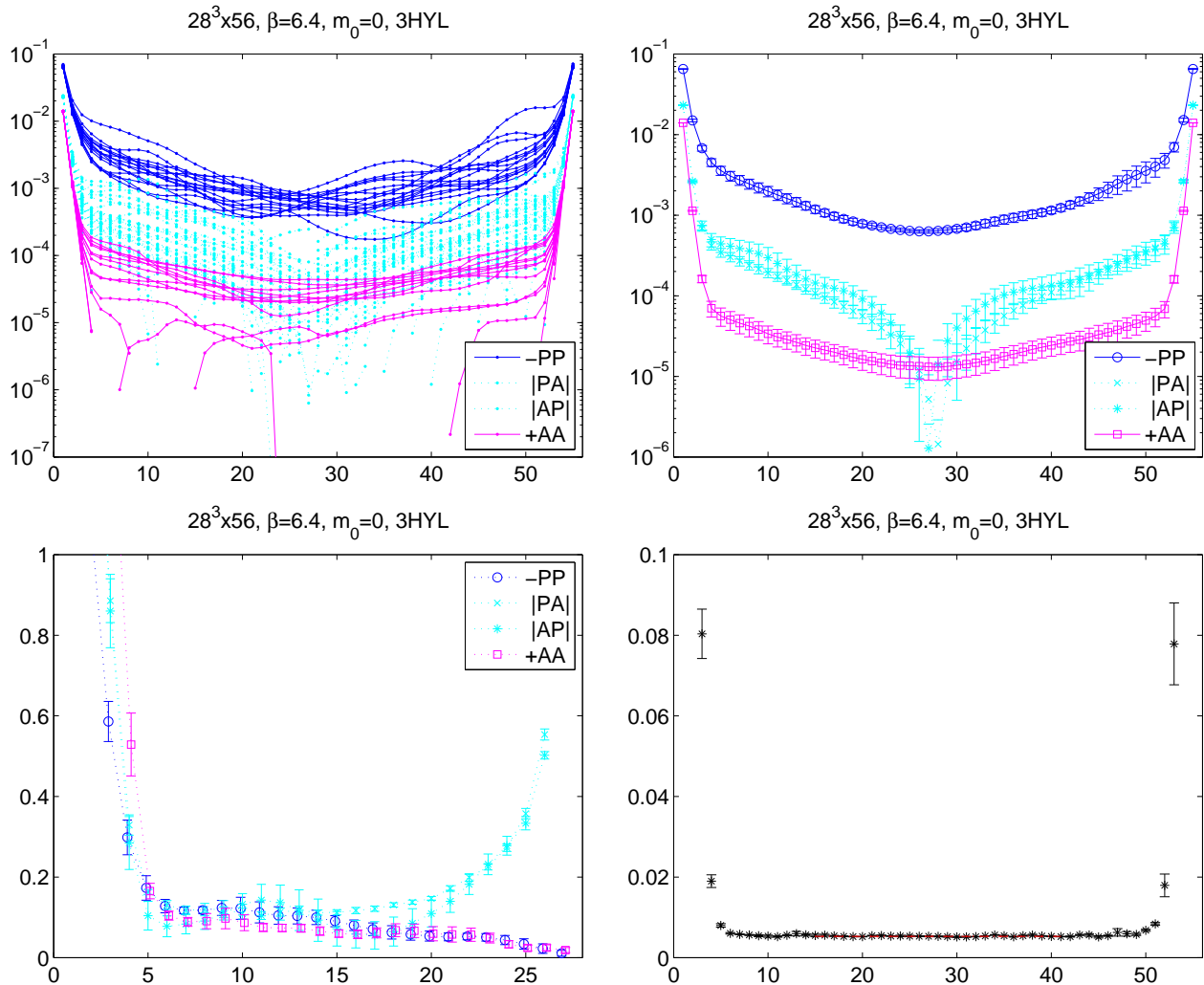


Figure 6: Same as in Fig. 5, but with 3 HYL smearing steps.

In Tab. 1 the values of the residual mass $am_{\text{res}}^{\text{PCAC}}$ at $am_0 = 0$ are summarized for 13 fermion actions at 5 couplings. The same (perturbatively equivalent) smearing parameters have been used as in Figs. 1 and 2, since we want to match on a common perturbative prediction (see below); results should not be interpreted as to give a fair comparison of the smearing recipes per se. Whether actions with $n_{\text{iter}} = 3 \dots 7$ suffer from “strong delocalization” effects (read: have bad scaling properties in some observables) is, at this moment, not clear. In state-of-the-art phenomenological studies one has several lattice spacings and thus means to check. The 7 HYL line has been included to indicate that there is no sign of a saturation of am_{res} versus n_{iter} in the range studied. The main message from Tab. 1 is rather encouraging; the LOG smearing defines a clover action with surprisingly good chiral symmetry properties. So far residual masses $am_{\text{res}} \simeq 10^{-3}$ have only been achieved with domain-wall fermions [14].

With Tab. 1 the main test has been completed, but it is still interesting to compare the data to the prediction from 1-loop fat-link perturbation theory. To lowest order the residual mass am_{res} relates to the frequently quoted critical mass am_{crit} through

$$m_{\text{res}} = \frac{|m_{\text{crit}}|}{Z_A} \frac{Z_P}{Z_S} \quad (15)$$

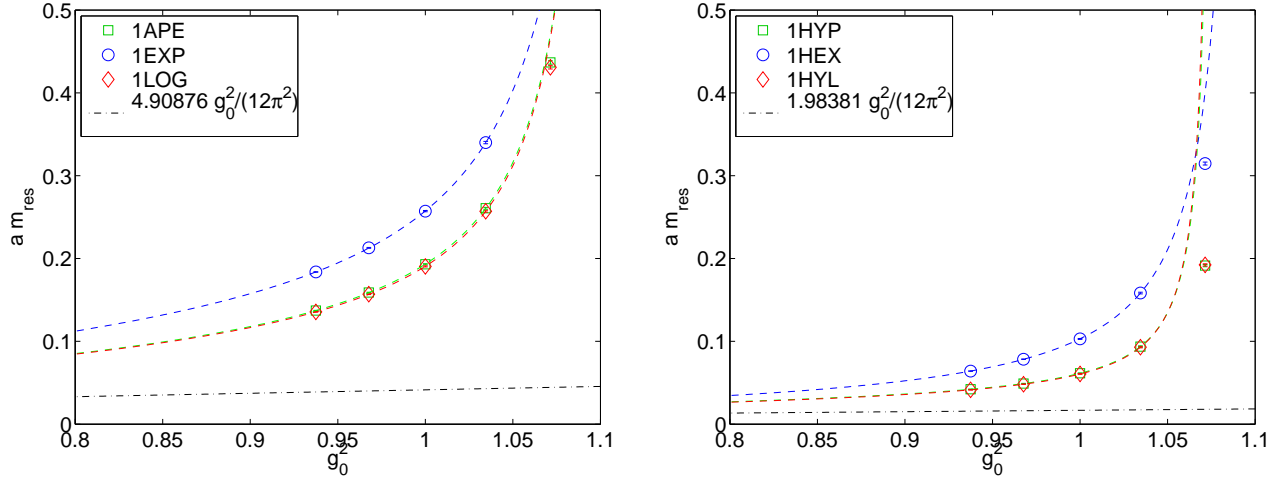


Figure 7: Graphical representation of the results of Tab. 1 for $n_{\text{iter}} = 1$ without (left) and with (right) hypercubic nesting. The common 1-loop prediction for each panel is shown as a straight dash-dotted line and is used as a constraint in fitting the data with $\beta \geq 5.8$ to the ansatz (17).

	c_0	c_1	c_2	c_3
1 APE	[4.90876]	0.40140	-0.95201	-0.90361
1 HYP	[1.98381]	-0.05780	-0.68221	-0.92911
1 EXP	[4.90876]	1.15872	-1.51175	-0.89583
1 HEX	[1.98381]	-0.03521	-0.43517	-0.91397
1 LOG	[4.90876]	0.39395	-0.95340	-0.90421
1 HYL	[1.98381]	-0.09322	-0.65284	-0.92974
3 APE	[0.77096]	0.27440	-0.74716	-0.92960
3 EXP	[0.77096]	0.64259	-0.90602	-0.92456
3 LOG	[0.77096]	0.25769	-0.72616	-0.92955

Table 2: Summary of the coefficients in the fit (17) for the 9 actions where c_0 is known in PT.

but the perturbative expansion $Z_X = 1 + O(g_0^2)$ means that at leading order there is no difference between am_{res} and am_{crit} . Thus we may directly take the result from [5] for our parameters

$$am_{\text{res}} = \frac{g_0^2}{16\pi^2} C_F S = \frac{g_0^2}{12\pi^2} \begin{cases} 4.90876 & (1 \text{ APE/EXP/LOG, } c_{\text{SW}} = 1) \\ 1.98381 & (1 \text{ HYP/HEX/HYL, } c_{\text{SW}} = 1) \\ 0.77096 & (3 \text{ APE/EXP/LOG, } c_{\text{SW}} = 1) \end{cases} \quad (16)$$

and confront it with the data. In Fig. 7 the data with $n_{\text{iter}} = 1$ are plotted against $g_0^2 = 6/\beta$. Since we are outside the regime where (16) is adequate it is natural to use the rational ansatz

$$am_{\text{res}} = \frac{g_0^2}{12\pi^2} c_0 \frac{1 + c_1 g_0^2 + c_2 g_0^4}{1 + c_3 g_0^2} \quad (17)$$

to fit the data, where the perturbative constraint (16) is built in by setting $c_0 = S$. The results of the fits to the data at $\beta \geq 5.8$ are summarized in Tab. 2. With these values in hand, the residual mass for any of these 9 actions can be accurately predicted in the range $\beta \geq 5.8$.

Finally it is interesting to convert the residual masses into physical units and to $(\overline{MS}, 2 \text{ GeV})$ conventions. In the first step we use again the formula from [13]; the result is shown in Tab. 3.

$(\beta, L/a)$	(5.6, 08)	(5.8, 12)	(6.0, 16)	(6.2, 20)	(6.4, 28)
1 LOG	0.9914(46)	0.9421(41)	1.0223(34)	1.1584(32)	1.3203(28)
1 HYL	0.4425(30)	0.3406(30)	0.3254(26)	0.3559(17)	0.4039(17)
3 LOG	0.4538(33)	0.3146(35)	0.2642(30)	0.2632(20)	0.2794(29)
3 HYL	0.1601(25)	0.0906(33)	0.0590(36)	0.0502(19)	0.0515(14)
7 HYL	0.0698(18)	0.0401(22)	0.0215(25)	0.0150(18)	0.0135(14)

Table 3: Same as Tab. 1, but converted to r_0 units, based on the formula for r_0/a given in [13].

$(\beta, L/a)$	(5.6, 08)	(5.8, 12)	(6.0, 16)	(6.2, 20)	(6.4, 28)
1 LOG	388(18)	381(17)	424(14)	489(13)	565(12)
1 HYL	165(11)	131(12)	129(10)	144(07)	166(07)
3 LOG	166(12)	119(13)	103(12)	105(08)	113(11)

Table 4: Same as Tab. 3, but converted to MeV and $(\overline{\text{MS}}, \mu = 2 \text{ GeV})$, based on Z_m from (18).

Assuming $r_0 = 0.5 \text{ fm}$, the second step is performed by means of $m^{\overline{\text{MS}}}(\mu) = Z_m(a\mu)m^{\text{PCAC}}(a^{-1})$, and we use the 1-loop perturbative prediction [as usual, up to $O(g_0^4)$ contributions]

$$Z_m = Z_S^{-1} = \left(1 - \frac{g_0^2}{3\pi^2} \left[\frac{z_S}{3} - \log(a^2\mu^2)\right]\right)^{-1} = 1 + \frac{g_0^2}{3\pi^2} \left[\frac{z_S}{3} - \log(a^2\mu^2)\right] \quad (18)$$

with the ingredients $z_S = 4.11106$ for 1 APE/EXP/LOG, $z_S = -1.43930$ for 3 APE/EXP/LOG and $z_S = -0.03678$ for 1 HYP/HEX/HYL from [5]. The results are shown in Tab. 4. Assuming that $M_\pi = 140 \text{ MeV}$ corresponds to $m^{\overline{\text{MS}}}(2 \text{ GeV}) = 4 \text{ MeV}$ we can now estimate the pion mass by multiplying 140 MeV with the square-root of $m^{\overline{\text{MS}}}(2 \text{ GeV})/(4 \text{ MeV})$. In fact, since Z_m is so close to 1, even an estimate based on the bare PCAC mass might be accurate to 10% or so. In case of the 3 HYL action it predicts $M_\pi \simeq 320 \text{ MeV}$ for $\beta = 6.4$, in fair agreement with the result from the effective mass plot. In case of the 7 HYL action the effective mass plot cannot be used as a check, but the estimate $M_\pi \simeq 160 \text{ MeV}$ might still be accurate within 20 MeV. Note finally that – with $m_0 = 0$ or $\kappa = 1/8$ fixed – all of this has been achieved in a regime (to be precise: at the edge of the regime) where we are safe against “exceptional configurations”.

6 Towards full QCD with the RHMC algorithm

With the tests of the LOG/HYL smearing in the quenched case completed, it seems worth while to spend a first thought one how one would use this smearing in full QCD.

The driving ingredient in a HMC algorithm is the molecular dynamics evolution which is determined by the so-called HMC force. Let D_m be an arbitrary undoubled fermion action, implicitly dependent on the “thin” gauge links U . The pseudofermion action is defined as

$$S_{\text{pf}} = \langle \phi | M^{-1/2} | \phi \rangle = \int \phi^\dagger(x) M^{-1/2}(x, y) \phi(y) d^4x d^4y, \quad M = D_m^\dagger D_m > 0 \quad (19)$$

where ϕ denotes a boson field with the spinor and color components of a standard Dirac flavor. We choose $N_f = 1$ for full generality; the version for even N_f is even simpler. The HMC force, finally, is defined as minus the derivative of S_{pf} with respect to the thin links [7]. The standard

way to proceed is to make use of the fact that the p -th order diagonal rational approximation of $x^{-1/2}$ over the relevant spectral range admits a partial fraction formulation [7]

$$x^{-1/2} \simeq \alpha_0 + \sum_{k=1}^p \frac{\alpha_k}{x + \beta_k} \quad (20)$$

with $\alpha_k > 0$ ($k=1\dots p$) and $0 < \beta_1 < \dots < \beta_p$. As a result, the pseudo-fermion force is given by

$$F_{\text{pf}} = -S'_{\text{pf}} = \sum_{k=1}^p \alpha_k \langle \phi | (M + \beta_k)^{-1} M' (M + \beta_k)^{-1} | \phi \rangle \quad (21)$$

where the prime denotes the variation w.r.t. a single element of the gauge field $A_\mu^a(x + \hat{\mu}/2)$, defined as a Gell-Mann component of $\log(U_\mu(x))$. In other words, what is needed to work out S'_{pf} is the derivative of M w.r.t. the gauge field. In explicit terms this is

$$M' = \frac{dM}{dA_\mu^a} = \frac{dD_m^\dagger}{dA_\mu^a} D_m + D_m^\dagger \frac{dD_m}{dA_\mu^a} = (D_m^\dagger)' D_m + D_m^\dagger (D_m)' \quad (22)$$

where the derivatives $(D_m^\dagger)'$ and $(D_m)'$ follow as a product of the variation of the chosen fermion action under a change of the “fat” links, times the inner derivative [15]. In the very end, the variation $dS_{\text{pf}}/dA_\mu^a(x + \hat{\mu})$ combines both types¹ of derivatives. The former is standard, except that in the result a replacement $U \rightarrow U^{\text{LOG}}$ is needed. The latter is specific to the chosen smearing recipe and hence deserves a closer look.

We restrict ourselves to the “trace-free” logarithm (8). The product rule (64) yields

$$\begin{aligned} \frac{\partial U_\mu^{\text{LOG}}(x)^c}{\partial U_\nu(y)^c} &= (U_\mu(x)' \otimes I_3) \cdot \frac{\partial}{\partial U_\nu(y)} \left\{ \exp\left(\frac{\alpha}{2(d-1)} \sum_{\pm\rho \neq \mu} \text{tflog}[U_\rho(x) U_\mu(x + \hat{\rho}) U_\rho^\dagger(x + \hat{\mu}) U_\mu^\dagger(x)]\right)^c \right\} \\ &+ I_3 \otimes \exp\left(\frac{\alpha}{2(d-1)} \sum_{\pm\rho \neq \mu} \text{tflog}[U_\rho(x) U_\mu(x + \hat{\rho}) U_\rho^\dagger(x + \hat{\mu}) U_\mu^\dagger(x)]\right) \cdot I_9 \delta_{\mu,\nu} \delta_{x,y} \end{aligned} \quad (23)$$

$$\frac{\partial U_\mu^{\text{LOG}}(x)^c}{\partial U_\nu^\dagger(y)^c} = (U_\mu(x)' \otimes I_3) \cdot \frac{\partial}{\partial U_\nu^\dagger(y)} \left\{ \exp\left(\frac{\alpha}{2(d-1)} \sum_{\pm\rho \neq \mu} \text{tflog}[U_\rho(x) U_\mu(x + \hat{\rho}) U_\rho^\dagger(x + \hat{\mu}) U_\mu^\dagger(x)]\right)^c \right\} \quad (24)$$

and analogously for the daggered fat-links. Here we use the tensor notation where the l.h.s. is a 9×9 matrix with $\partial U_\mu^{\text{LOG}}(x)_{ij} / \partial U_\nu(y)_{kl}$ in the $3(j-1) + i$ -th row and $3(l-1) + k$ -th column. In other words, $U_\mu^{\text{LOG}}(x)$ and $U_\nu(y)$ are “reshaped” into 9×1 column vectors, and then the derivative of the p -th element of the first with respect to the q -th element of the second appears in position (p, q) . Likewise, on the r.h.s. the derivative is a 9×9 matrix, and $U_\mu(x)$ has been “blown up” by tensoring with the identity such that the two 9×9 matrices would multiply according to standard matrix multiplication rules. Some details of the underlying formalism

¹We use the standard definition (with \tilde{U} denoting a generic fat link)

$$\frac{d(\cdot)}{dA_\mu^a} = \frac{\partial(\cdot)}{\partial A_\mu^a} + \frac{\partial(\cdot)}{\partial U_\nu} \frac{dU_\nu}{dA_\mu^a} + \frac{\partial(\cdot)}{\partial U_\nu^\dagger} \frac{dU_\nu^\dagger}{dA_\mu^a}, \quad \frac{\partial(\cdot)}{\partial U_\mu} = \frac{\partial(\cdot)}{\partial \tilde{U}_\nu} \frac{\partial \tilde{U}_\nu}{\partial U_\mu} + \frac{\partial(\cdot)}{\partial \tilde{U}_\nu^\dagger} \frac{\partial \tilde{U}_\nu^\dagger}{\partial U_\mu}, \quad \frac{\partial(\cdot)}{\partial U_\mu^\dagger} = \frac{\partial(\cdot)}{\partial \tilde{U}_\nu} \frac{\partial \tilde{U}_\nu}{\partial U_\mu^\dagger} + \frac{\partial(\cdot)}{\partial \tilde{U}_\nu^\dagger} \frac{\partial \tilde{U}_\nu^\dagger}{\partial U_\mu^\dagger}$$

in which the partial derivative w.r.t. a given link picks up only that link and not its hermitean conjugate, that is U_μ and U_μ^\dagger are considered independent with regard to partial differentiation.

have been collected in App. C. The task is now to collect the various pieces that come from the derivative of the exponential. Upon applying the chain rule (65) for matrix functions, I obtain

$$\frac{\partial}{\partial U_\nu(y)^c} \left\{ \exp\left(\frac{\alpha}{2(d-1)} \sum_{\pm\rho\neq\mu} \text{tflog}[U_\rho(x)U_\mu(x+\hat{\rho})U_\rho^\dagger(x+\hat{\mu})U_\mu^\dagger(x)]\right)^c \right\} = F_1 \cdot F_2 \cdot F_3 \quad (25)$$

$$\frac{\partial}{\partial U_\nu^\dagger(y)^c} \left\{ \exp\left(\frac{\alpha}{2(d-1)} \sum_{\pm\rho\neq\mu} \text{tflog}[U_\rho(x)U_\mu(x+\hat{\rho})U_\rho^\dagger(x+\hat{\mu})U_\mu^\dagger(x)]\right)^c \right\} = F_1 \cdot F_2 \cdot F_4 \quad (26)$$

where each factor

$$F_1 = \frac{\partial \exp(X)^c}{\partial X^c} \quad \text{evaluated at} \quad X = \frac{\alpha}{2(d-1)} \sum_{\pm\rho\neq\mu} \text{tflog}[U_\rho(x)U_\mu(x+\hat{\rho})U_\rho^\dagger(x+\hat{\mu})U_\mu^\dagger(x)]$$

$$F_2 = \frac{\alpha}{2(d-1)} \sum_{\pm\rho\neq\mu} \frac{\partial \text{tflog}(X)^c}{\partial X^c} \quad \text{evaluated at} \quad X = U_\rho(x)U_\mu(x+\hat{\rho})U_\rho^\dagger(x+\hat{\mu})U_\mu^\dagger(x)$$

$$\begin{aligned} F_3 &= [U_\rho^\dagger(x+\hat{\mu})U_\mu^\dagger(x)]' \otimes I_3 \cdot \frac{\partial (U_\rho(x)U_\mu(x+\hat{\rho}))^c}{\partial U_\nu(y)^c} \\ &= [U_\mu(x+\hat{\rho})U_\rho^\dagger(x+\hat{\mu})U_\mu^\dagger(x)]' \otimes I_3 \delta_{\nu,\rho} \delta_{x,y} + [U_\rho^\dagger(x+\hat{\mu})U_\mu^\dagger(x)]' \otimes U_\rho(x) \delta_{\mu,\nu} \delta_{x+\hat{\rho},y} \end{aligned}$$

$$\begin{aligned} F_4 &= I_3 \otimes [U_\rho(x)U_\mu(x+\hat{\rho})] \cdot \frac{\partial (U_\rho^\dagger(x+\hat{\mu})U_\mu^\dagger(x))^c}{\partial U_\nu^\dagger(y)^c} \\ &= U_\mu^\dagger(x)' \otimes [U_\rho(x)U_\mu(x+\hat{\rho})] \delta_{\nu,\rho} \delta_{x+\hat{\mu},y} + I_3 \otimes [U_\rho(x)U_\mu(x+\hat{\rho})U_\rho^\dagger(x+\hat{\mu})] \delta_{\mu,\nu} \delta_{x,y} \end{aligned}$$

is a 9×9 matrix, and similarly for the daggered fat-links. If the LOG smearing is iterated, several factors (23, 24) are lined up, each one evaluated with the appropriate argument.

For completeness, let us consider fat-link clover fermions, although this has been done before [15]. Introducing, for each term in (21), $|\eta_k\rangle = (M + \beta_k)^{-1}|\phi\rangle$ and $|\zeta_k\rangle = D_m|\eta_k\rangle$ we have

$$F_{\text{pf}} = -S'_{\text{pf}} = \sum_{k=1}^p \alpha_k \left[\langle \eta_k | (D_m^\dagger)' | \zeta_k \rangle + \langle \zeta_k | (D_m)' | \eta_k \rangle \right] \quad (27)$$

where we enjoy the benefits of dealing with a scalar function of a scalar argument (such that the full apparatus of App. C is not needed). From a glimpse at (12) it follows that

$$\frac{\partial S_{\text{pf,W}}}{\partial U_\mu^{\text{LOG}}(x)} = \frac{1}{2} \sum_{k=1}^p \alpha_k \text{Tr}_{\text{spin}} \left[\eta_k^\dagger(x+\hat{\mu})(\gamma_\mu + I)\zeta_k(x) - \zeta_k^\dagger(x)(\gamma_\mu - I)\eta_k(x+\hat{\mu}) \right] \quad (28)$$

where the layout of the color structure on the r.h.s. is just adapted to whichever convention on the l.h.s. is chosen. Similarly, from a glimpse at (13) it follows that

$$\frac{\partial S_{\text{pf,SW}}}{\partial U_\mu^{\text{LOG}}(x)} = \frac{c_{\text{SW}}}{2} \sum_y \sum_{k=1}^p \alpha_k \text{Tr}_{\text{spin}} \left[\eta^\dagger(y) \sigma_{\kappa\lambda} \frac{\partial F_{\kappa\lambda}^{\text{LOG}}(y)}{\partial U_\mu^{\text{LOG}}(x)} \zeta(y) + \zeta^\dagger(y) \sigma_{\kappa\lambda} \frac{\partial F_{\kappa\lambda}^{\text{LOG}}(y)}{\partial U_\mu^{\text{LOG}}(x)} \eta(y) \right]. \quad (29)$$

Upon putting the various expressions together, one has an analytic expression for the HMC force of a LOG-filtered clover (staggered, overlap, etc.) action. The generalization to the HYL smearing (10) follows by lining up several factors of (23, 24) [with restricted sums].

7 Modified gauge action and topological charge density

In the numerical investigations of this note the traditional Wilson gauge action

$$S_G = \frac{2N_c}{g_0^2} \sum_{x,\mu<\nu} \left\{ 1 - \frac{1}{N_c} \text{Re Tr}(U_{\mu\nu}(x)) \right\} \quad (30)$$

has been used. However, with the technical means to compute the matrix logarithm of the plaquette $U_{\mu\nu}(x) = U_\mu(x)U_\nu(x+\hat{\mu})U_\mu^\dagger(x+\hat{\nu})U_\nu^\dagger(x)$ in hand, two modifications are possible.

The first one concerns a constraint, to be added to whichever gauge action is used. Clearly, the discussion around (5-8) would have been much simpler, if we could be sure that there is no lattice in our ensemble with a single $U_{\mu\nu}(x)$ which has a non-trace-free principal logarithm. It can be shown that a sufficient condition for $\text{Tr log}(U_{\mu\nu}(x)) = 0$ is $\text{Re Tr}(U_{\mu\nu}(x)) > -1$. This suggests adding a piece which penalizes all plaquettes with $\text{Re Tr}(U_{\mu\nu}(x)) < 0$, without affecting those with $\text{Re Tr}(U_{\mu\nu}(x)) \geq 0$. Alternatively, one may directly test for $\text{Tr log}(U_{\mu\nu}(x)) = \pm 2\pi i$ and assign, in such a case, a prohibitive extra action. This point is summarized through

$$S_G \longrightarrow S_G + \begin{cases} +\frac{1}{\epsilon} \sum_{x,\mu<\nu} \theta(-r) \exp(1/r) & \text{with } r = \text{Re Tr}(U_{\mu\nu}(x)) \\ -\frac{1}{\epsilon} \sum_{x,\mu<\nu} [\text{Tr log}(U_{\mu\nu}(x))]^2 & \text{with } \epsilon \ll 1. \end{cases} \quad (31)$$

The second one concerns a modification of the ‘‘bulk’’ piece of the gauge action. Recalling that the rationale behind Wilson’s choice (30) is to come up with a simple recipe to produce a term $F_{\mu\nu}^2$ from $U_{\mu\nu} = \exp(ig_0 a F_{\mu\nu}) = 1 + ig_0 a^2 F_{\mu\nu} - \frac{1}{2} g_0^2 a^4 F_{\mu\nu}^2 - \dots$, it is tempting to generate $F_{\mu\nu}$ directly from the logarithm of the plaquette and square it explicitly. With $L_{\mu\nu}(x) = \text{tflog } U_{\mu\nu}(x)$ and $\bar{L}_{\mu\nu}(x) = \frac{1}{4}[L_{\mu\nu}(x) + L_{\mu\nu}(x-\hat{\mu}) + L_{\mu\nu}(x-\hat{\nu}) + L_{\mu\nu}(x-\hat{\mu}-\hat{\nu})]$ at hand, it appears that

$$S_G[U] = a^4 \sum_{x,\mu<\nu} \text{Tr}[F_{\mu\nu}(x)F_{\mu\nu}(x)] \doteq -\frac{1}{g_0^2} \sum_{x,\mu<\nu} \text{Tr}[\bar{L}_{\mu\nu}(x)\bar{L}_{\mu\nu}(x)] \quad (32)$$

would be a rather natural choice. Likely this gauge action defines a theory with good scaling properties, good rotational symmetry and nice overlap with the perturbative regime, as it is rather similar to the Manton action [16]. On the other hand, tunneling of the topological charge needs to be investigated, and clearly (32) is not as easy to simulate as the Wilson action (30).

Of course, the same modification may be applied to $F\tilde{F}$, too. This yields the expression

$$q[U] = \frac{a^4}{32\pi^2} \sum_{x,\mu\nu\rho\sigma} \epsilon_{\mu\nu\rho\sigma} \text{Tr}[F_{\mu\nu}(x)F_{\rho\sigma}(x)] \doteq -\frac{1}{32\pi^2 g_0^2} \sum_{x,\mu\nu\rho\sigma} \epsilon_{\mu\nu\rho\sigma} \text{Tr}[\bar{L}_{\mu\nu}(x)\bar{L}_{\rho\sigma}(x)] \quad (33)$$

for the bare topological charge density. Unlike in the previous case, we do not expect this to be much better than the usual clover-leaf expression for the topological charge density, since in that case it is standard to perform an averaging of the anti-hermitean part of the plaquette.

In the same spirit, it seems natural to define the clover action through

$$D_{\text{SW}}(x, y) = D_{\text{W}}(x, y) - \frac{c_{\text{SW}}}{2ig_0} \sum_{\mu<\nu} \sigma_{\mu\nu} \bar{L}_{\mu\nu} \delta_{x,y} \quad (34)$$

instead of (13) [where $F_{\mu\nu}$ follows from the anti-hermitean part of the same 4 plaquettes which enter $\bar{L}_{\mu\nu}$]. Again, at least with some filtering, this change will be rather insignificant.

8 Summary and outlook

The purpose of this paper has been to define and test a smearing which is applicable, in the context of the HMC algorithm, to studies of full QCD. The testing has been restricted to pure gauge theory observables and to clover fermions in quenched QCD, but it is clear that the main lesson concerns the fermion formulation per se.

The key idea behind this LOG smearing is to do the “averaging” in the Lie algebra, such that one would end up with a smeared (“fat”) link which is naturally in the original gauge group. This is a clear advantage if one intends to use such fat-links in observables which are sensitive to the structure of the gauge group (e.g. Polyakov loops), but it might also simplify calculations in fermionic systems (e.g. by providing a more direct connection to perturbation theory). Whenever a single LOG smearing (8) is not enough, it seems advisable to use the hypercubic nesting to define the HYL smeared links (10).

Tests in the pure gauge theory have shown that the new LOG smearing is at least as effective at suppressing UV fluctuations as known alternatives. From a practical viewpoint the LOG smearing seems to have an advantage in having a rather broad “near-optimal” region, i.e. good results do not require any fine-tuning of the smearing parameter.

An important point is that the LOG/HYL smearing yields a fat-link which is differentiable with respect to the thin links it is built from. This makes it a useful ingredient in defining a UV-filtered fermion action which can be used to study full QCD with the HMC algorithm. The tests in the quenched theory have shown quite convincing results, though most of the good properties of such actions are not specific to the LOG/HYL recipes. These smearings are efficient in the sense that modest parameters and/or iteration counts lead to clover-fermions with quite acceptable chiral properties. It seems that, upon iterating the smearing, arbitrarily small residual masses can be attained. The smallest value found, $am_{\text{res}} = 0.0014(1)$ with 7 HYL steps at $\beta = 6.4$, is in a regime which, without smearing, can only be accessed by domain-wall fermions [14]. It seems noteworthy that these results have been obtained with non-negative bare mass where one is immune against “exceptional configurations”. An obvious continuation of the current work would be to compare the scaling properties of such actions against mildly filtered or unfiltered (“thin link”) varieties. From Fig. 6 one sees that the correlators of highly smeared actions at small quark mass become sensitive to individual instantons and/or other topological objects and get rather fuzzy. Likely, this is the flipside of any fermion action with good chiral properties. The present tests have focused on the residual mass, as this is the simplest observable sensitive to chiral symmetry breaking. Perhaps a study of the spectral gap of the hermitean Wilson/clover operator with LOG/HYL-filtering would be useful, too.

Wilson fermions have been out of fashion for over a decade, since in the original formulation chiral symmetry is broken in a rather severe way, and standard Symanzik improvement alone does not bring a major change in this respect. It seems almost guaranteed that, upon combining a clover term with a modest amount of link-fattening (e.g. two HYL steps), the clover action is rendered a competitive choice for pushing towards $M_\pi = 140$ MeV in full QCD.

Acknowledgments:

I would like to thank Anna Hasenfratz for raising my interest in differentiable fat-link recipes and Ferenc Niedermayer for a series of most enjoyable discussions. Computations have been performed on stand-alone PCs with 4GB memory. I’m indebted to Markus Moser and Matthias Nyfeler for creating temporary swap space. This work was supported by the Swiss NSF.

A Matrix exponential, matrix logarithm and more

Among the main concepts for computing matrix valued functions on the computer, viz.

- (i) eigenvalue and eigenfunction based routines
- (ii) clever use of the Cayley-Hamilton theorem
- (iii) iterative methods

a combination of (i) and (ii) often yields the most efficient implementation. Nonetheless, it turns out that iterative methods – though originally designed to deal with medium-size full and huge sparse systems – represent a good choice already for 3×3 matrices, since they are easy to implement, numerically stable, and still reasonably fast in terms of CPU time. Below a robust implementation of the matrix exponential and the matrix logarithm is described.

A.1 Matrix exponential with iterative methods

The matrix exponential of an arbitrary $m \times m$ matrix A is defined through (with $A^0 = I$)

$$\exp(A) = \sum_{k=0}^{\infty} \frac{A^k}{k!} \quad (35)$$

since this series has infinite convergence range. A general recipe to speed up the convergence is known as the “scaling and squaring” method. It is based on the trivial observation

$$\exp(A) = [\exp(A/2^n)]^{2^n} \quad (36)$$

which is paraphrased as “take $\exp(A/2)$ and square it, and nest this n times”. The point is, of course, that $A/2$ has smaller eigenvalues (or singular values) than A , making the power series for $A/2$ converge faster than the one for A . Clearly, theorems may be derived for the optimal choice of n . However, in practice it is often sufficient to start with a reasonable n_{\min} , and to increase it until the result is stable. An implementation of the estimator $E_n(\cdot)$, in which also the precision of the rational approximation $R_n(\cdot)$ is gradually increased, reads

$$\begin{aligned} & E_{n_{\min}-1} = I \\ & \text{for } n = n_{\min} : \infty \\ & \quad S_n = A/2^n, R_n = [\sum_{k=0}^{2n} \frac{1}{k!} (S_n/2)^k] [\sum_{k=0}^{2n} \frac{1}{k!} (-S_n/2)^k]^{-1}, E_n = (R_n)^{2^n} \\ & \quad \text{if } \|E_n - E_{n-1}\| < \epsilon \text{ exit} \\ & \text{end} \end{aligned} \quad (37)$$

where $\|\cdot\|$ is any matrix norm and ϵ is usually chosen slightly larger than the machine precision. An aside: In a HMC algorithm one needs to calculate $\exp(A)$ for $A \in su(3)$. In order to guarantee reversibility, one demands that $E(-A)$ is the exact inverse of $E(A)$, even with a low grade $E(\cdot)$. Our representation $R_n(A) = [I + A/2 + \dots][I - A/2 + \dots]^{-1}$, and thus $E_n(\cdot)$, is of this form.

A.2 Matrix logarithm with iterative methods

The matrix logarithm of a non-singular $m \times m$ matrix A is, in general, not unique. However, if A has no eigenvalues on the closed negative real axis, then there is one solution to the equation $\exp(X) = A$ for which all eigenvalues x_i of X satisfy $-\pi < \text{Im}(x_i) < \pi$ ($i = 1, \dots, m$), and this

solution is called the principal logarithm of A and denoted $\log(A)$. Since there is no power series representation of $\log(A)$ which converges in the entire cut plane, the usefulness of an “inverse scaling and squaring” approach [17], based on the identity

$$\log(A) = \log(A^{1/2^n}) \cdot 2^n \quad (38)$$

is evident. It may be paraphrased as “take the square root, compute the logarithm, double it, and nest this n times”. Hence this approach leaves us with the problem to compute, with high precision, the principal square root of an arbitrary matrix A , but the gain is that the argument of the innermost (“reduced”) logarithm is, for large enough n , close to the identity.

For the square root it is convenient to use an iterative method, too. The Newton iteration

$$X_{k+1} = \frac{1}{2}(X_k + AX_k^{-1}), \quad X_0 = A \quad (39)$$

with $\lim_{k \rightarrow \infty} X_k = A^{1/2}$ has good theoretical properties, but its poor numerical stability renders it useless in practice [18]. Fortunately, the Denman-Beavers iteration [19] for A with a spectrum contained in the cut complex plane (i.e. with no non-positive real eigenvalue)

$$\begin{aligned} Y_{k+1} &= \frac{1}{2}(Y_k + Z_k^{-1}), & Y_0 &= A \\ Z_{k+1} &= \frac{1}{2}(Z_k + Y_k^{-1}), & Z_0 &= I \end{aligned} \quad (40)$$

has the quadratic convergence pattern

$$\lim_{k \rightarrow \infty} Y_k = A^{1/2}, \quad \lim_{k \rightarrow \infty} Z_k = A^{-1/2}$$

and is stable against round-off errors [18]. Throughout this appendix it is understood that the inverse is determined via a Gauss elimination (with pivoting whenever needed) and hence exact to machine precision. In particular, if one is interested only in $A^{1/2}$ (or $A^{-1/2}$), the product form of the Denman-Beavers iteration [18]

$$\begin{aligned} Y_{k+1} &= \frac{1}{2}Y_k(I + M_k^{-1}), & Y_0 &= A \\ Z_{k+1} &= \frac{1}{2}(I + M_k^{-1})Z_k, & Z_0 &= I \\ M_{k+1} &= \frac{1}{4}(M_k + 2I + M_k^{-1}), & M_0 &= A \end{aligned} \quad (41)$$

with the line for Z_{k+1} (or for Y_{k+1}) omitted and the quadratic convergence pattern from above (plus $\lim_{k \rightarrow \infty} M_k = I$, and hence $\|M_k - I\| < \epsilon$ as a natural exit criterion) proves superior. The reason is that only one inverse is required and the matrix to be inverted is, after a few steps, so close to the identity that no pivoting is needed (which is primarily useful when dealing with large matrices on massively parallel systems). In general, one will also use the scaling idea to accelerate this product form of the Denman-Beavers iteration (see [18] for details), but in our case $\det(A) = 1$ implies that no scaling is needed in this step. Note that (40, 41) are non-standard in the sense that the matrix A does not show up in the iteration step.

For the second ingredient, the logarithm of a matrix close to the identity, one option is to utilize a diagonal rational approximation of $\log(1 - x)$, for instance one of

$$\begin{aligned} r_{11}(x) &= \frac{-2x}{2-x} \\ r_{22}(x) &= \frac{-6x+3x^2}{6-6x+x^2} \\ r_{33}(x) &= \frac{-60x+60x^2-11x^3}{60-90x+36x^2-3x^3} \\ r_{44}(x) &= \frac{-2940x+4410x^2-1820x^3+175x^4}{2940-5880x+3780x^2-840x^3+42x^4} \end{aligned}$$

with $X = 1 - A$. Here it is understood that the numerator and denominator are at least evaluated by means of the Horner scheme, but the larger m in $r_{mm}(\cdot)$, the more it pays to use a sophisticated method [20]. An alternative representation, which is easier to implement, is

$$\log(Z) = 2\left\{(Z-1)(Z+1)^{-1} + \frac{1}{3}[(Z-1)(Z+1)^{-1}]^3 + \frac{1}{5}[(Z-1)(Z+1)^{-1}]^5 + \dots\right\} \quad (42)$$

which is appropriate for $\text{Re}(z_i) \geq 0, z_i \neq 0 (\forall i)$. In our situation this condition is met after the first square root has been evaluated. An aside: If the inversion is exact, upon feeding (42) with Z^{-1} one obtains exactly the negative of what one gets with Z , in spite of the truncation.

Putting things together, one may either opt for the more elaborate algorithm of Ref. [18]

$$\begin{aligned} &Y^{(0)} = A \\ &\text{for } i = 1 : \infty \\ &\quad \text{choose } k_i \text{ according to Theorem 5.1 of Ref. [18]} \\ &\quad M_0 = Y^{(i-1)}, Y_0 = Y^{(i-1)} \\ &\quad \text{for } k = 0 : k_i - 1 \\ &\quad\quad Y_{k+1} = Y_k(I + M_k^{-1})/2, M_{k+1} = (2I + M_k + M_k^{-1})/4 \\ &\quad \text{end} \\ &\quad M^{(i)} = M_{k_i}, Y^{(i)} = Y_{k_i}, n = i \\ &\quad \text{if } \|I - Y^{(k)}\| \leq \frac{1}{2} \text{ and (7.5) of Ref. [18] satisfied with } m_n \leq 8 \text{ exit} \\ &\quad \text{end} \\ &\quad \text{form the Pade approximant } X = r_{m_n m_n}(I - Y^{(n)}) \\ &\quad \text{rescale and correct through } X = X2^n - \sum_{i=1}^n (M^{(i)} - I)2^{i-1} \end{aligned} \quad (43)$$

which uses a Pade approximant of maximum order [8/8] for the reduced logarithm, or one may decide to stay with the simpler algorithm (starting again with a fixed $n_{\min} \geq 2$)

$$\begin{aligned} &L_{n_{\min}-1} = 0 \\ &\text{let } S_{n_{\min}-1} \text{ be the result of } n_{\min}-1 \text{ nestings of (41), each one run to machine precision} \\ &\text{for } n = n_{\min} : \infty \\ &\quad \text{let } S_n \text{ be the result of (41) with } A = S_{n-1}, \text{ again run to machine precision} \\ &\quad R_n = 2 \sum_{k=1}^{4n} \frac{1}{2k-1} [(S_n - I)(S_n + I)^{-1}]^{2k-1} \\ &\quad L_n = 2^n R_n \\ &\quad \text{if } \|L_n - L_{n-1}\| < \epsilon \text{ exit} \\ &\quad \text{end} \end{aligned} \quad (44)$$

which is similar in spirit to (37) for the matrix exponential. In the second case one may choose to increment n by more than one unit. In these implementations no property of $SU(3)$ matrices has been exploited. Accordingly, if the argument is known to be a special unitary matrix, it is useful to check that the matrix logarithm is anti-hermitean and traceless modulo $2\pi i$.

A.3 Higher matrix roots with iterative methods

A problem in our approach of nesting n inverse scaling and squaring steps is that $n-1$ times we use the output of a square-root operation as input for the next one. In this form round-off errors will accumulate and the approximant of the 2^n -fold root will deviate from $A^{1/2^n}$ by an error which grows exponentially with n . It then is natural to look for a post-iteration which renders the result of the root-cascade exact. We thus face the question how to compute the fourth (eighth, etc.) root of a matrix, if a relatively good initial guess is already known.

Having a reasonable guess for $A^{1/p}$, we have, via a simple inversion, also a guess for $A^{-1/p}$, and vice versa. The simplest strategy is to run the (stable) Newton postiteration

$$X_{k+1} = \frac{p+1}{p}X_k - \frac{1}{p}X_k^{1+p}A, \quad X_0 \simeq A^{-1/p} \quad (45)$$

with the approximate inverse of the p -th root as a starting value, and then invert the result. Note that this recursion is expensive; it requires $n+2 = \log_2(p) + 2$ matrix multiplications per step. Still, since in a post-iteration typically just 1 or 2 steps are needed, this is acceptable.

A.4 Post-iteration of the matrix logarithm

Alternatively, one might stay with the uncorrected n -fold square root cascade, and correct, instead, the final logarithm. The standard approach for this is to use the Newton iteration

$$X_{n+1} = X_n - I + \frac{1}{2}(e^{-X_n}A + Ae^{-X_n}) \quad (46)$$

where we have opted for the symmetric version. Again, the individual step is expensive (a new exponential is needed in each step), but for a post-iteration this is acceptable.

A.5 Matrix logarithm for unitary arguments

For unitary argument the principal matrix logarithm is purely anti-hermitean, $\log(U) = iH$ with $H = H^\dagger$ and $\text{spec}(H) \in]-\pi, \pi[$. Based on the experience with (and some of the ingredients from) the general algorithm (44) it is straight-forward to devise an algorithm tailored to yield the matrix logarithm of a unitary argument U [21].

At the beginning one has $\cos(H)$ and $i \sin(H)$, defined as the hermitean and anti-hermitean parts of U . One may think of accumulating knowledge about subsequent half-angle sine and cosine functions, such that in the end one has $\sin(H/2^n)/\cos(H/2^n) = \tan(H/2^n)$ and by means of an arctan-representation which is valid for small arguments one gets $H/2^n$ and thus H .

In fact, two tricks ease our task. The first one is the identity

$$\tan(H/4) = \sin(H) \left[1 + \cos(H) + \sqrt{2} [1 + \cos(H)]^{1/2} \right]^{-1} \quad (47)$$

which allows us to directly jump to the quarter-angle operator, at the expense of a single Denman-Beavers iteration (41). The second one is again based on $H/4$ having a spectrum in the open interval $]-\pi/4, \pi/4[$; now $Z = \tan(H/4)$ is just in the range of convergence of

$$\arctan(Z) = Z - \frac{1}{3}Z^3 + \frac{1}{5}Z^5 - \dots = \sum_{k=0}^{\infty} \frac{(-1)^k}{2k+1} Z^{2k+1} \quad (||Z|| < 1). \quad (48)$$

As a result, no nested square-root scheme is needed, and the only exit criterion is concerned with the absolutely convergent series (48). In practice it proves useful to monitor the numerical convergence of the series, and to post-iterate with (46) if needed.

A.6 Unitary projection with iterative methods

The ability to calculate $A^{-1/2}$ is also useful for the polar decomposition that is needed in the projection step of the traditional APE or HYP smearing procedure. Given a non-unitary $V_\mu(x)$ [the linear combination inside the wavy bracket in (2)], one proceeds in two steps. Usually, one thinks of first projecting to $U(3)$, and then adjusting the determinant

$$W_\mu(x) = V_\mu(x)[V_\mu^\dagger(x)V_\mu(x)]^{-1/2}, \quad U_\mu(x) = W_\mu(x)/\det^{1/3}[W_\mu(x)] \quad (49)$$

where $W_\mu(x)$ is the unitary part of $V_\mu(x)$, which is unique if $V_\mu(x)$ is nonsingular. In practice it is often a better choice to reverse the order, i.e. to compute

$$W_\mu(x) = V_\mu(x)/\det^{1/3}[V_\mu(x)], \quad U_\mu(x) = W_\mu(x)[W_\mu^\dagger(x)W_\mu(x)]^{-1/2} \quad (50)$$

to speed up the iterative polar decomposition, if the latter is done without rescaling.

One way to compute the unitary part is via the quadratically convergent Newton iteration

$$X_{k+1} = \frac{1}{2}(\gamma_k X_k + \gamma_k^{-1}(X_k^\dagger)^{-1}), \quad X_0 = A \quad (51)$$

with $\lim_{k \rightarrow \infty} X_k = A(A^\dagger A)^{-1/2}$, where $\gamma_k = |\det(X_k)|^{-1/2}$, $\gamma_k = (\sigma_{\min}(X_k)\sigma_{\max}(X_k))^{-1/2}$, or $\gamma_k = (||X_k^{-1}||/||X_k||)^{1/2}$ (with the Frobenius norm) represent typical choices for the scaling parameter. Upon first adjusting the determinant to 1, i.e. upon using $A = V_\mu(x)/\det^{1/3}[V_\mu(x)]$, the choice $\gamma_k = 1$ ($\forall k$) becomes quite efficient.

Another option is to use the product form of the Denman-Beavers iteration (41) for $A^{-1/2}$ with $A = V_\mu^\dagger(x)V_\mu(x)/\det^{1/3}[V_\mu^\dagger(x)V_\mu(x)]$ and leftmultiply the result with $V_\mu(x)/\det^{1/3}(V_\mu(x))$. Again, due to $\det(A)=1$, this is efficient without further rescaling.

Finally, it is worth pointing out that, for arbitrary given V , the matrix $P_{U(N)} = V(V^\dagger V)^{-1/2}$ maximizes $\text{Re tr}(V^\dagger U)$ over all unitary U , but the $SU(N)$ matrix $P_{\det=1} P_{U(N)} V = P_{U(N)} P_{\det=1} V$ does not maximize $\text{Re tr}(V^\dagger U)$ over all special unitary matrices. This is of interest in the context of a direct overrelaxation in $SU(N)$, as discussed in [22].

A.7 Eigenvalue based logarithm of a unitary matrix

For an arbitrary 3×3 matrix A , the Vieta theorem for the characteristic polynomial yields

$$\lambda_1 + \lambda_2 + \lambda_3 = \text{Tr}(A), \quad \lambda_1\lambda_2 + \lambda_1\lambda_3 + \lambda_2\lambda_3 = \det(A)\text{Tr}(A^{-1}), \quad \lambda_1\lambda_2\lambda_3 = \det(A) \quad (52)$$

and for a unitary matrix this simplifies to

$$\lambda_1 + \lambda_2 + \lambda_3 = \text{Tr}(U) , \quad \lambda_1\lambda_2 + \lambda_1\lambda_3 + \lambda_2\lambda_3 = \text{Tr}(U)^* , \quad \lambda_1\lambda_2\lambda_3 = \det(U) \quad (53)$$

where the star denotes complex conjugation.

As a result, the eigenvalue based method for computing the matrix logarithm of a unitary 3×3 matrix U starts with the coefficients of the characteristic polynomial $x^3 + ax^2 + bx + c = 0$, that is with $a = -\text{Tr}(U)$, $b = \text{Tr}(U)^* = -a^*$, $c = -\det(U)$. Next, form the complex quantities $Q = a^2/9 - b/3$ and $R = a^3/27 - ab/6 + c/2 = aQ/3 - ab/18 + c/2$. If Q and R are both real and $R^2 < Q^3$, then the cubic equation has three real roots. In the $SU(3)$ case, this means either $\lambda_1 = \lambda_2 = \lambda_3 = 1$, or one eigenvalue $+1$ and two -1 . Otherwise, form $A = -[R + \sqrt{R^2 - Q^3}]^{1/3}$ [with the complex square-root chosen such that $\text{Re}(R^* \sqrt{R^2 - Q^3}) > 0$] and $B = Q/A$. With these at hand, the solution (Cardano, 1545)

$$x_1 = (A+B) - \frac{a}{3} , \quad x_2 = -\frac{1}{2}(A+B) - \frac{a}{3} + i\frac{\sqrt{3}}{2}(A-B) , \quad x_3 = -\frac{1}{2}(A+B) - \frac{a}{3} - i\frac{\sqrt{3}}{2}(A-B) \quad (54)$$

is written in such a way as to minimize round-off errors [23].

Having the eigenvalues, the pertinent eigenvectors may be found through solving a linear system; the eigenvector $v^{(i)}$ ($i = 1..3$) is simply the solution of $(U - \lambda_i I)v^{(i)} = 0$. Building on the fact that $S = U - \lambda_i I$ is singular, a convenient choice for the components of $v^{(i)}$ is the minors of, e.g., the first row: $v_1^{(i)} = S_{22}S_{33} - S_{23}S_{32}$, $v_2^{(i)} = S_{23}S_{31} - S_{21}S_{33}$, $v_3^{(i)} = S_{21}S_{32} - S_{22}S_{31}$. Here, it is assumed that the second and third row are linearly independent [but, of course, any row is in the span of the other two]. Whenever the maximum degeneracy is two-fold, there is at least one such choice which yields a non-zero eigenvector.

With the normalized eigenvectors at hand, the principal logarithm of U would be $\log(U) = \sum_{i=1}^3 \log(\lambda_i) v^{(i)} v^{(i)\dagger}$. The virtue of the eigenvalue based approach is that it gives us the means to identify the ‘‘troublesome’’ λ_i whenever the principal logarithm has a non-zero trace. Assume the trace is $+2\pi i$; in that case $\log(\lambda_1) + \log(\lambda_2) + \log(\lambda_3) = 2\pi i$. Identify the $\log(\lambda_i)$ with the largest imaginary part [they all lie on the imaginary axis]. Set $\mu_i = \log(\lambda_i) - 2\pi i$ for that i and $\mu_j = \log(\lambda_j)$ for the other two. The trace-free logarithm is then $\text{tflog}(U) = \sum_{i=1}^3 \mu_i v^{(i)} v^{(i)\dagger}$, with an obvious generalization to the case where the trace of the principal logarithm is $-2\pi i$. In mathematical terms this procedure is equivalent to shifting the cut of the logarithm such that one of the eigenvalues lies on the second Riemann sheet.

Finally, note that this procedure is in marked contrast to the naive approach of subtracting one third of the trace from the principal logarithm, as is done in (6, 7). This naive recipe amounts to shifting each $\log(\lambda_i)$ by $\pm 2\pi i/3$.

A.8 Appendix summary

While faster algorithms exist to compute the matrix exponential, the principal logarithm and the projection to $SU(3)$, the iterative methods described in this appendix yield numerically stable results with 64-bit machine precision after $O(< 10)$ steps. Moreover, the possibility to warrant exact HMC reversibility, even if one opts for a lower precision, seems attractive. For the non-principal logarithm used in (8), the eigenvalue based method seems most convenient.

B Tricks for EO-preconditioned BCG γ_5 solver

In (full or quenched) QCD one solves the Dirac equation $Dx = b$ for a given right-hand side b . A key feature of the clover D is that it couples nearest neighbors, apart from a mass and a clover contribution which do not hop at all. Accordingly, upon labeling the sites in a checkerboard (“even-odd”) fashion, the problem takes a block-offdiagonal form, except for the generalized mass contribution which remains site-diagonal. Hence D can be block- LU -factorized [24]

$$D = \begin{pmatrix} D_{ee} & D_{eo} \\ D_{oe} & D_{oo} \end{pmatrix} = L\tilde{D}U = \begin{pmatrix} 1 & 0 \\ D_{oe}D_{ee}^{-1} & 1 \end{pmatrix} \begin{pmatrix} \star & 0 \\ 0 & \star \end{pmatrix} \begin{pmatrix} 1 & D_{ee}^{-1}D_{eo} \\ 0 & 1 \end{pmatrix} \quad (55)$$

where the Schur complements L and U are easily inverted (by flipping the sign of the block-offdiagonal piece) and the block-diagonalized \tilde{D} takes the form

$$\tilde{D} = \begin{pmatrix} 1 & 0 \\ -D_{oe}D_{ee}^{-1} & 1 \end{pmatrix} \begin{pmatrix} D_{ee} & D_{eo} \\ D_{oe} & D_{oo} \end{pmatrix} \begin{pmatrix} 1 & -D_{ee}^{-1}D_{eo} \\ 0 & 1 \end{pmatrix} = \begin{pmatrix} D_{ee} & 0 \\ 0 & D_{oo} - D_{oe}D_{ee}^{-1}D_{eo} \end{pmatrix}. \quad (56)$$

As a result, the original problem is split into three parts: (i) left-multiply the source with L^{-1} , that is define the new source c with $c_e = b_e$ and $c_o = b_o - D_{oe}D_{ee}^{-1}b_e$; (ii) solve the non-trivial block problem $\tilde{D}_{oo}y_o = c_o$ and the trivial one $y_e = \tilde{D}_{ee}^{-1}c_e$; (iii) left-multiply the solution with U^{-1} , that is obtain x from y through $x_o = y_o$ and $x_e = y_e - D_{ee}^{-1}D_{eo}y_o$.

It is worth pointing out two peculiarities of the clover case. First, contrary to the Wilson case, where D_{oo} and D_{ee} are constants, they now happen to be site diagonal, that is they are composed of V little 12×12 matrices [for $SU(3)$ gauge group, with V the number of sites]. In the chiral representation, the latter are further reduced to two 6×6 matrices. Still, this has a severe impact on the memory requirement. In order to have a fast forward-application routine, it is customary to allocate an array which contains all 6×6 matrices needed. This amounts to a vector of $72V$ complex entries, to be compared to the $36V$ complex entries of the gauge field and the $6V$ complex entries of a half-vector.

Second, the non-trivial problem in step (ii) may be traded for the more symmetric version $(1 - D_{oo}^{-1}D_{oe}D_{ee}^{-1}D_{eo})y_o = D_{oo}^{-1}c_o$ with a slightly lowered condition number [25, 26]. On the other hand, the reduced operator $D_{\text{red}} = \frac{1}{2}(D_{oo} - D_{oe}D_{ee}^{-1}D_{eo})$ is γ_5 -hermitean; thus the original version can be mapped into $H_{\text{red}}y_o = \frac{1}{2}\gamma_5c_o$ with the hermitean, indefinite $H_{\text{red}} = \gamma_5D_{\text{red}}$. In addition, it implies that the operator $D_{\text{sym}} = 2(1 - D_{oo}^{-1}D_{oe}D_{ee}^{-1}D_{eo})$ enjoys a γ_5D_{oo} -hermiticity, that is $D_{\text{sym}}^\dagger = 2(1 - \gamma_5D_{oe}D_{ee}^{-1}D_{eo}D_{oo}^{-1}\gamma_5) = \gamma_5D_{oo}D_{\text{sym}}D_{oo}^{-1}\gamma_5$. Similarly, the other symmetric operator, that follows from D_{sym} by eo-flipping the suffixes, is γ_5D_{ee} -hermitean (and has an identical spectrum). In all these considerations it is assumed that the little 6×6 matrices are inverted beforehand, so that D_{ee}^{-1} (and, if needed, D_{oo}^{-1}) are known.

The operator D_{red} being γ_5 -hermitean, it is tempting to use the BCG γ_5 -algorithm [27] to solve the reduced system in step (ii) above. As is well known, with finite-precision arithmetics BCG γ_5 is prone to suffer from instabilities, and this holds true after EO-preconditioning, too. The instability is mainly due to the indefinite scalar products [with a γ_5 between the two vectors] genuine to this algorithm. Such an object may happen to be quite small in absolute magnitude, while the individual terms in the sum are not. In practice it is, nonetheless, observed that the algorithm performs quite convincingly, if the following three “tricks” are used:

1. perform the summation in the $(\cdot, \gamma_5 \cdot)$ -type scalar products in quadruple precision [the products to be summed over are still computed in standard double precision]

2. recompute the true residue much more frequently than one would do in an algorithm without indefinite scalar products, e.g. every 10-th step instead of every 100-th step
3. keep track of the vector which gave, so far, the smallest true residue, and restart, if certain conditions are met, from this vector.

Evidently, devising a good set of conditions is important. In some of the simulations presented in this article, BCG_{γ_5} was restarted if the norm of the actual residue was three orders of magnitude above the best residue encountered so far and, at the same time, the last restart would date back at least 500 steps. It turned out that a better condition is to demand that the minimum residue would persist for 500 steps and the last restart would date back at least 1500 steps. It is advisable to code the routine such that – in case the required residual norm would not be reached within the maximum number of steps – it would return the best approximation encountered and another algorithm (e.g. CGNE) would take over. In the simulations presented in this article this has never happened.

C Tensor calculus and chain rule for matrix functions

In this appendix a convenient notation is introduced whereupon the chain rule for matrix valued functions looks like the usual chain rule for scalar functions. The material is mostly taken from [28], but restricted to the case of square matrices, since this is all that we need.

Considering a function $Y(X)$ with X and Y both $N \times N$ matrices, the derivative $\partial Y / \partial X$ is conveniently represented as a $N^2 \times N^2$ matrix, since it is supposed to contain information on how each element of Y depends on each element of X . In the mathematical literature three conventions regarding the ordering of its entries may be found, but only one of them allows for a simple-looking generalization of the chain rule for scalar functions.

For definiteness, let us recall some standard mathematical notation. A matrix A is represented as $A = (a_{ij}e_i^j)$ with the usual summation convention for repeated indices within a bracket. Here, e_i^j is an $N \times N$ matrix with zeros everywhere except for the place in row i and column j . The Kronecker product of A and $B = (b_{kl}e_k^l)$ is then a $N^2 \times N^2$ matrix

$$A \otimes B = (\{a_{ij}b_{kl}\}e_{ik}^{jl}) \quad (57)$$

which is constructed by blowing up A and plugging B into every partition (multiplied with the element of the former A). Accordingly, the product $a_{ij}b_{kl}$ is found in position (p, q) of the new matrix with $p = (i-1)N + k$ and $q = (j-1)N + l$. In fact, this is the reason for the notation used in (57), where only information on the ordering of covariant indices among themselves (and ditto for contravariant indices) is retained, but no information on the relative ordering of covariant and contravariant indices. One is invited to read (ik) as the new row index and (jl) as the new column index, with the breakdown into row and column number as given above. When traveling through the new matrix, i and j move slowly, while k and l move rapidly. Upon tensoring (57) with a matrix $C = (c_{mn}e_m^n)$ the old layout is again blown up and we arrive at

$$A \otimes B \otimes C = (\{a_{ij}b_{kl}c_{mn}\}e_{ikm}^{jln}) \quad (58)$$

with the row and column multiindices (ikm) and (jln) translating into $p = ((i-1)N + k - 1)N + m$ and $q = ((j-1)N + l - 1)N + n$, respectively. The important point is that these Kronecker

products form an associative algebra, that is

$$(A \otimes B \otimes C)(D \otimes E \otimes F) = (AD \otimes BE \otimes CF). \quad (59)$$

In the first definition the derivative of Y with respect to X is a partitioned matrix $[\partial Y / \partial x_{ij}]$ whose (i, j) partition is put together by taking the derivatives $\partial y_{kl} / \partial x_{ij}$ for all entries of Y . In other words, the layout is similar to that of $X \otimes Y$, that is

$$\left[\frac{\partial Y}{\partial x_{ij}} \right] = \left(\frac{\partial y_{kl}}{\partial x_{ij}} e_{ik}^{jl} \right). \quad (60)$$

In the second definition the derivative of Y with respect to X is a partitioned matrix $[\partial y_{kl} / \partial X]$ whose (k, l) partition is put together by taking the derivatives $\partial y_{kl} / \partial x_{ij}$ for all entries of X . In other words, the layout is similar to that of $Y \otimes X$, that is

$$\left[\frac{\partial y_{kl}}{\partial X} \right] = \left(\frac{\partial y_{kl}}{\partial x_{ij}} e_{ki}^{lj} \right). \quad (61)$$

In the third definition the derivative of Y with respect to X is obtained by first reshaping both matrices into $N^2 \times 1$ column vectors, denoted X^c and Y^c , respectively. In this step the second column is appended to the first one, and so on. Then the derivative of the p -th element of X^c with respect to the q -th element of Y^c is stored in position (p, q) . In other words, the layout is similar to that of $Y^c \otimes (X^c)' = (\{x_{ij} y_{kl}\} e_{lk}^{ji})$, with $'$ denoting the transposition, that is

$$\left[\frac{\partial Y^c}{\partial X^c} \right] = \left(\frac{\partial y_{kl}}{\partial x_{ij}} e_{lk}^{ji} \right). \quad (62)$$

When comparing these definitions one notices that the first two differ only by the order among the covariant indices and among the contravariant indices. Therefore, the two can be mapped into each other by means of transpositions. By contrast, the third definition differs from the previous two in a more profound manner; for this change covariant indices need to be converted into contravariant indices and vice versa. Another notation for this third definition, which sometimes occurs in the literature, is $\partial \text{vec} Y / \partial \text{vec}' X = \partial \text{vec} Y / \partial (\text{vec} X)'$.

We start with having a look into the product rule with this third definition. Let $Y(X)$ and $Z(X)$ be two matrix valued functions which depend on X . According to the standard rules, the derivative of the product $W = YZ = (w_{kn} e_k^n)$ with respect to X is

$$\left[\frac{\partial W^c}{\partial X^c} \right] = \left(\frac{\partial w_{kn}}{\partial x_{ij}} e_{nk}^{ji} \right) = \left(\frac{\partial y_{kl}}{\partial x_{ij}} z_{ln} e_{nk}^{ji} \right) + \left(y_{km} \frac{\partial z_{mn}}{\partial x_{ij}} e_{nk}^{ji} \right) \quad (63)$$

where $w_{kn} = (y_{ko} z_{on})$ has been used. On the other hand, the derivative of Y with respect to X is the $N^2 \times N^2$ matrix (62), which cannot be multiplied with Z , unless the latter is tensored with the identity I to have the right dimension. However, standard algebra gives

$$\begin{aligned} (Z \otimes I) \left[\frac{\partial Y^c}{\partial X^c} \right] &= \left(z_{mn} \delta_{pq} e_{mp}^{nq} \right) \delta_{nl} \delta_{qk} \left(\frac{\partial y_{kl}}{\partial x_{ij}} e_{lk}^{ji} \right) = \left(z_{ml} \delta_{pk} e_{mp}^{lk} \right) \left(\frac{\partial y_{kl}}{\partial x_{ij}} e_{lk}^{ji} \right) = \left(\frac{\partial y_{kl}}{\partial x_{ij}} z_{ml} e_{mk}^{ji} \right) \\ (I \otimes Y) \left[\frac{\partial Z^c}{\partial X^c} \right] &= \left(\delta_{pq} y_{kl} e_{pk}^{ql} \right) \delta_{qn} \delta_{lm} \left(\frac{\partial z_{mn}}{\partial x_{ij}} e_{nm}^{ji} \right) = \left(\delta_{pn} y_{km} e_{pk}^{nm} \right) \left(\frac{\partial z_{mn}}{\partial x_{ij}} e_{nm}^{ji} \right) = \left(y_{km} \frac{\partial z_{mn}}{\partial x_{ij}} e_{nk}^{ji} \right) \end{aligned}$$

and therefore the product rule for matrix derivatives is seen to take the form

$$\left[\frac{\partial(YZ)^c}{\partial X^c} \right] = (Z' \otimes I) \left[\frac{\partial Y^c}{\partial X^c} \right] + (I \otimes Y) \left[\frac{\partial Z^c}{\partial X^c} \right]. \quad (64)$$

In fact, upon generalizing the size of X to $M \times N$, and that of Y and Z to $P \times Q$ and $Q \times R$, respectively, the l.h.s. of (64) is an $PR \times MN$ matrix. At the same time the first term on the r.h.s. is the product of a $PR \times PQ$ matrix (with $I = I_P$) and a $PQ \times MN$ matrix. And the second term is the product of a $PR \times QR$ matrix (with $I = I_R$) and a $QR \times MN$ matrix. Hence either term, and the r.h.s. in total, is of size $PR \times MN$, in perfect agreement with the l.h.s.

The main reason why it pays to choose the layout (62) is that this definition allows for a neat extension of the standard chain rule. Let $Z = Z(Y)$ be a matrix valued function of Y and $Y = Y(X)$ a matrix valued function of X . With similar manipulations as above it follows that

$$\left[\frac{\partial Z^c}{\partial X^c} \right] = \left[\frac{\partial Z^c}{\partial Y^c} \right] \left[\frac{\partial Y^c}{\partial X^c} \right] \quad (65)$$

where the l.h.s. is a $QR \times MN$ matrix and the r.h.s. is a $QR \times PQ$ times a $PQ \times MN$ matrix. Therefore, also this rule remains valid for arbitrarily shaped source and target matrices. Note that, with any of the other definitions of the matrix derivative, one would be forced to introduce a clumsy “star product” which does not obey the usual rules of matrix multiplication.

It is worth noticing that the similarity to the chain rule for scalar functions is somehow limited, since the derivative of $\exp(\cdot)$ and $\log(\cdot)$ is not given by $\exp(\cdot)$ and $(\cdot)^{-1}$, respectively [which would be matrices of inappropriate size]. Due to the infinite series in the definition of $\exp(X)$, the (k, l) element of the exponential depends on each x_{ij} . Accordingly, $\partial \exp(X)^c / \partial X^c$ is a full $N^2 \times N^2$ matrix, and a similar statement holds true for $\partial \log(X)^c / \partial X^c$. Still, with

$$\frac{\partial(X^n)^c}{\partial X^c} = \frac{\partial(X^{n-1} \cdot X)^c}{\partial X^c} = (X' \otimes I) \frac{\partial(X^{n-1})^c}{\partial X^c} + I \otimes X^{n-1} \quad (66)$$

for $I = I_N$ it follows that the derivative of the n -th power can be written in compact form

$$\frac{\partial(X^n)^c}{\partial X^c} = \sum_{\ell=0}^{n-1} (X' \otimes I)^{n-1-\ell} (I \otimes X^\ell) = \sum_{\ell=0}^{n-1} (X')^{n-1-\ell} \otimes X^\ell \quad (67)$$

and similarly the derivative of the inverse of a matrix $Y = Y(X)$ is given by

$$\frac{\partial(Y^{-1})^c}{\partial X^c} = -(Y^{-1'} \otimes Y^{-1}) \frac{\partial Y^c}{\partial X^c}. \quad (68)$$

Thanks to the exponential being given by a globally convergent power series, it follows that

$$\frac{\partial \exp(X)^c}{\partial X^c} = \sum_{n=1}^{\infty} \frac{1}{n!} \sum_{\ell=0}^{n-1} (X')^{n-1-\ell} \otimes X^\ell \quad (69)$$

and the chain rule (65) says that the inverse of it, if it exists, is $\partial \log(Y)^c / \partial Y^c$ at $Y = \exp(X)$.

With the formalism presented in this appendix the HMC force for an arbitrary fat-link action can be worked out in a way which relies only on the standard matrix multiplication law and may, as a result, benefit from optimized linear algebra subroutines.

References

- [1] K. Symanzik, Nucl. Phys. B **226**, 187 (1983).
- [2] T.A. DeGrand, A. Hasenfratz and T.G. Kovacs [MILC Collaboration], hep-lat/9807002. C.W. Bernard and T. DeGrand, Nucl. Phys. Proc. Suppl. **83**, 845 (2000) [hep-lat/9909083]. M. Stephenson, C. DeTar, T.A. DeGrand and A. Hasenfratz, Phys. Rev. D **63**, 034501 (2001) [hep-lat/9910023].
- [3] S. Dürr and C. Hoelbling, Phys. Rev. D **72**, 071501 (2005) [hep-ph/0508085].
- [4] C. Bernard *et al.* [MILC Collaboration], PoS **LAT2006**, 163 (2006) [hep-lat/0609053].
- [5] S. Capitani, S. Dürr and C. Hoelbling, JHEP **0611**, 028 (2006) [hep-lat/0607006] and PoS **LAT2006**, 157 (2006) [hep-lat/0609059].
- [6] S. Dürr *et al.*, PoS **LAT2007**, 115 (2007) [0710.4769, hep-lat].
- [7] For a guide to the literature see: M.A. Clark, PoS **LAT2006**, 004 (2006) [hep-lat/0610048].
- [8] M. Falcioni, M.L. Paciello, G. Parisi and B. Taglienti, Nucl. Phys. B **251**, 624 (1985). M. Teper, Phys. Lett. B **183**, 345 (1987). M. Albanese *et al.* [APE Collaboration], Phys. Lett. B **192**, 163 (1987).
- [9] C. Morningstar and M.J. Peardon, Phys. Rev. D **69**, 054501 (2004) [hep-lat/0311018].
- [10] A. Hasenfratz, R. Hoffmann and S. Schaefer, JHEP **0705**, 029 (2007) [hep-lat/0702028].
- [11] A. Hasenfratz and F. Knechtli, Phys. Rev. D **64**, 034504 (2001) [hep-lat/0103029].
- [12] B. Sheikholeslami and R. Wohlert, Nucl. Phys. B **259**, 572 (1985).
- [13] S. Necco and R. Sommer, Nucl. Phys. B **622**, 328 (2002) [hep-lat/0108008].
- [14] C. Allton *et al.* [RBC and UKQCD Collabs.], Phys. Rev. D **76**, 014504 (2007) [hep-lat/0701013].
- [15] W. Kamleh, D.B. Leinweber and A.G. Williams, Phys. Rev. D **70**, 014502 (2004) [hep-lat/0403019].
- [16] N.S. Manton, Phys. Lett. B **96**, 328 (1980).
- [17] C.S. Kenney and A.J. Laub, SIAM J. Matrix Anal. Appl. **10**, 191 (1989).
- [18] S.H. Cheng, N.J. Higham, C.S. Kenney and A.J. Laub, SIAM J. Matrix Anal. Appl. **22**, 1112 (2001).
- [19] E.D. Denman and A.N. Beavers Jr., Appl. Math. and Comput. **2**, 63 (1976).
- [20] N.J. Higham, SIAM J. Matrix Anal. Appl. **22**, 1126 (2001).
- [21] S.H. Cheng, N.J. Higham, C.S. Kenney and A.J. Laub, Proceedings of the Fourteenth International Symposium of Mathematical Theory of Networks and Systems, Perpignan, France (2000).
- [22] P. de Forcrand and O. Jahn, hep-lat/0503041.
- [23] W.H. Press, S.A. Teukolsky, W.T. Vetterling, B.P. Flannery, Numerical recipes in C, 2nd edition, Cambridge University Press, 1992.
- [24] T.A. DeGrand, Comput. Phys. Commun. **52**, 161 (1988).
- [25] K. Jansen and C. Liu, Comput. Phys. Commun. **99**, 221 (1997) [hep-lat/9603008].
- [26] T. Chiarappa *et al.*, hep-lat/0609023.
- [27] P. de Forcrand, Nucl. Phys. Proc. Suppl. **47**, 228 (1996) [hep-lat/9509082].
- [28] D.S.G. Pollock, Linear Algebra and its Applications **67**, 169-193 (1985).